



**PHOTOLUMINESCENCE SPECTRA OF GALLIUM ARSENIDE  
NANOWIRE AND CONFINEMENT EFFECT**

*By*

*Leta Tesfaye Jule*

*SUBMITTED IN PARTIAL FULFILMENT OF THE  
REQUIREMENTS FOR THE DEGREE OF  
MASTER OF SCIENCE IN PHYSICS*

*AT*

*ADDIS ABABA UNIVERSITY  
ADDIS ABABA, ETHIOPIA*

*June 2011*

*©Copyright by Leta Tesfaye, 2011*

**ADDIS ABABA UNIVERSITY  
DEPARTMENT OF  
PHYSICS**

***The undersigned hereby certify that they have read and recommend to the School of Graduate Studies for acceptance a thesis entitled “PHOTOLUMINESCENCE SPECTRA OF GALLIUM ARSENIDE NANOWIRE AND CONFINEMENT EFFECT ” by Leta Tesfaye in partial fulfillment of the requirements for the degree of Master of Science in Physics.***

***Dated :-***

***Supervisor: Dr. Tesgera Bedassa***

***Examiners:***

**ADDIS ABABA UNIVERSITY**

**Date: June 2011**

**Author: Leta Tesfaye Jule**

**Title: PHOTOLUMINESCENCE SPECTRA OF GALLIUM ARSENIDE  
NANOWIRE AND CONFINEMENT EFFECT ”**

**Department: Physics**

**Degree: M. Sc**

**Convocation: June**

**Year: 2011**

*Permission is herewith granted to Addis Ababa University to circulate and to have copied for non-commercial purposes, at its discretion, the above title upon the request of individuals or institutions.*

*Signature of Author*

**THE AUTHOR RESERVES OTHER PUBLICATION RIGHTS, AND NEITHER THE THESIS NOR EXTENSIVE EXTRACTS FROM IT MAY BE PRINTED OR OTHERWISE REPRODUCED WITHOUT THE AUTHOR'S WRITTEN PERMISSION.**

**THE AUTHOR ATTESTS THAT PERMISSION HAS BEEN OBTAINED FOR THE USE OF ANY COPYRIGHTED MATERIAL APPEARING IN THIS THESIS (OTHER THAN BRIEF EXCERPTS REQUIRING ONLY PROPER ACKNOWLEDGEMENT IN SCHOLARLY WRITING) AND THAT ALL SUCH USE IS CLEARLY ACKNOWLEDGED.**

# Table of Contents

<b>Table of Contents.....</b>	<b>i</b>
<b>List of Figures .....</b>	<b>ii</b>
<b>Acknowledgements.....</b>	<b>iii</b>
<b>Abstract.....</b>	<b>iv</b>
<b>1.Introduction.....</b>	<b>1</b>
<b>1.1 Energy quantization and band gap of gallium arsenide nanowire.....</b>	<b>4</b>
<b>1.2 Light emitting property of GaAs nanostructures.....</b>	<b>5</b>
<b>1.3 Oxide-assisted growth and optical characterization of gallium arsenide nanowires.....</b>	<b>7</b>
<b>1.4 Research Objectives.....</b>	<b>10</b>
1.5 Scopes of the Study.....	10
<b>2.Bulk and nanostructured semiconductor systems.....</b>	<b>11</b>
<b>2.1 Semiconductors.....</b>	<b>11</b>
<b>2.2 Semi-conducting nanoparticles and Optical Properties .....</b>	<b>13</b>
<b>2.3 Energy Bands and Gaps of Semiconductors.....</b>	<b>14</b>
<b>2.4 Electron transport in direct gap semiconductors , GaAs.....</b>	<b>15</b>
<b>2.5 Quantum wells,wires and dots .....</b>	<b>16</b>
<b>2.6 Preparation of quantum nanostructures.....</b>	<b>16</b>
2.6.1 Quantum Dots .....	17
2.6.2 Quantum wires (nanowires).....	18
2.6.3 Quantum Wells .....	19
<b>2.7 Photoluminescence.....</b>	<b>20</b>
<b>3. Methods of the study.....</b>	<b>21</b>
<b>3.1 Effective mass approximation.....</b>	<b>21</b>
<b>4. Result and Discussion.....</b>	<b>23</b>
<b>4.1 Outstanding models .....</b>	<b>31</b>
<b>4.1.1 Quantum confinement.....</b>	<b>31</b>
<b>4.1.2 Other schemes.....</b>	<b>31</b>
<b>4.1.3 comparison with experiment.....</b>	<b>32</b>
<b>5. Conclusion.....</b>	<b>37</b>
<b>5.1 Application.....</b>	<b>38</b>
<b>5.2 Challenges.....</b>	<b>39</b>
<b>5.3 Future outlook.....</b>	<b>40</b>
<b>6. References.....</b>	<b>41</b>

## List of figures

<b>Figure 1.</b> Electronic density of states of semiconductors with 3, 2, 1 and 0 degrees of freedom for electron propagation. 2, 1 and 0 degrees of freedom referred to as quantum wells, quantum wires and quantum dots respectively. ....	4
<b>Figure 2.</b> Raman spectra recorded at room temperature for different samples (A(at 3000 c),B(at 5000 c), C(at 7000 c )(adapted from 8).....	6
<b>Figure 3.</b> <i>Temperature dependence photoluminescence spectra of untreated GaAs, sample A and C</i> .....	6
<b>Figure 4.</b> Typical SEM image of GaAs nanowires. Inset shows EDX spectrum taken from GaAs nanowires.....	7
<b>Figure.5</b> <i>Room-temperature Raman spectrum (a) of GaAs nanowires and PL spectra (b) of GaAs nanowires and GaAs bulk crystal</i> .....	8
<b>Figure.6</b> Typical photoluminescence spectra observed from the three types of nanowires at T = 4.2 K. The spectra have been obtained from single wires under illumination at 632.8 nm with a power density of 2.5 W / cm <sup>2</sup> . The emission energy shifts from 1.51 eV down to 1.43 eV depending on the growth conditions which result in different proportion of wurtzite and zinc-blende GaAs. ....	9
<b>Figure 7</b> <i>a) Gallium arsenide quantum well on a substrate; (b) quantum wire and quantum dot formed by lithography</i> .....	17
<b>Figure 8.</b> Theoretical PL spectra based on the above equation , The solid line depicts the case when $k=5$ ( i.e., $m=2$ , $x=2$ , and $\beta = 0$ ). The broken line is plotted with $m=2$ , $x=2$ , and $\beta =6$ ( $k=-1$ ), and shows a blue shift. The dotted line corresponds to $m=2$ , $x=1.4$ , and $\beta =0$ . The plots are normalized, with $c=485.816$ eV/Å <sup>2</sup> .....	24
<b>Figure 9.</b> The dependence of the peak position $\Delta E_p$ on the mean crystallite size, assuming a normal distribution of dots with $\sigma=5A^0$ $x=2$ .The broken line at the bottom ( $m=3$ , $\beta=0$ ) shows an extremely weak variation in energy with size. The dotted line at the top ( $m=3$ , $\beta=6$ ) shows a strong dependence which is supra-quadratic. The distribution in the crystallite sizes results in considerable deviation from a simple $c/d^x$ variation,which is depicted by the solid line.....	27

**Figure 10.** Emission photoluminescence spectra of Q-GaAs nanowire/4ep.....30

**Figure 11.** PL versus Energy in GaAs nanowire from the experimental data.....33

**Figure 13.** Intensity versus ramanshift for the three samples of GaAs nanowire discussed from the experimental datas for our comparison. And normalized intensity versus energy and wave length.....35

**Figure 14** Energy versus wave vector in GaAs. .... 35.

## **Acknowledgements**

*I would like to thank my advisor and instructor Dr. Tesgera Bedassa for his many suggestions, and Prof. Manlevi for his constant support and providing the necessary materials throughout my graduate study and during the course of this thesis. I am also thankful to the department of Physics for their co-operation during my M. Sc studies.*

*I would like to thank my family for their invaluable support. Without them, none of this would have been possible. I would also like to thank my friends, who were by my side morally throughout my study and also helped edit this thesis. Finally Ministry of education(MOE) for sponsoring my graduate study.*

## ABSTRACT

In this paper we present a detailed analysis of the atomic, optical and electronic structures of GaAs nanowires grown along [111]. and we reveal interesting trends among variation gap and size, oscillator strength and size, quantum confinement and size of particle and and the overall photoluminescence of GaAs nanowire and observing their spectra by varying diameters.

The size (d) dependence of photoluminescence from nanocrystalline GaAs nanowire semiconductors is examined. The overall luminescence is determined by two distinct physical mechanisms:

- 1) the variation of the semiconductor gap with size d (typically  $\sim 1/d^\alpha$ ,  $\alpha > 1$  and
- 2) the variation of the oscillator strength  $f_{osc}$  with size (typically  $1/d^\beta$ ,  $5 \leq \beta \leq 6$ ) We present an analytical framework to understand the luminescence line shape based on the above two mechanisms, taking no recourse to computational simulations. We show that the peak energy varies with the mean particle size  $d_0$  as  $d_0^{-\beta}$ , where  $\beta$  is an effective exponent determined by the disorder in the system.

Semiconductor nanowires have occupied the center of scientific interest because of their unique electronic nature. Among the group III-V compound, the gallium arsenide nanowire have been the focus of this research due to their importance in constructing fast microelectric devices. The electronic structures of gallium arsenide nanowire were studied.

Our work shows that the presence of disorder can shift the photoluminescence peak position. In the absence of a strong size dependence of the oscillator strength, the peak is redshifted. This allows one to assume reasonable values for the excitonic energy ( $\sim 50$  meV). However, if the oscillator strength is strongly dependent on size, the peak blue shift so large excitonic energies are needed to explain the disparity.

Attempts to understand the experimental data on the basis of calculation, and curve fitting model are the core method of this thesis.

However, the surface states associated with the surface atoms having two dangling bonds in zinc-blende stacking occur in the band gap and can decrease the band gap to change the nanowire from semiconducting to metallic state. These nanowires become semiconducting upon hydrogen passivation. Even if the band gap of some nanowires decreases with increasing diameter and hence reveals the quantum confinement effect, generally the band-gap variation is rather complex, and depends on the type and geometry, diameter, type of relaxation, and also whether the dangling bonds of surface atoms are saturated with hydrogen.



# Chapter 1

## 1.Introduction

The development of semiconductor physics undoubtedly embodies one of the most outstanding evidences of human progress. Maybe Michael Faraday himself could not expect that his discovery of a negative temperature coefficient of resistance in silver sulphide in 1834 was going to be the starting point of a long but successful process whose achievements make available today systems allowing an amazingly high degree of external control. His finding indeed provided the very first sign that control on the concentration of charge carriers could be attained in semiconductor materials. Control on the precise number of electrons at the single-electron level is nowadays achievable in structures making use of semiconductor quantum dots .

An obvious milestone of semiconductor physics is the revolutionary discovery of the transistor effect by Shockley, Bardeen and Brattain in 1947 . Semiconductor transistors are today the building blocks of the circuitry underlying the whole modern electronics. About a decade later, the latter received an even stronger impetus with the introduction of the integrated circuit chipable to host a large number of tiny individual transistors. Since then, the number of transistors for a single chip has nearly quadrupled every three years, this trend being pushed by the insatiable demand for increasing functionality per unit of area.

The requirement of higher integration capability has motivated the development of more and more advanced fabrication techniques with increasing level of accuracy up to the point that present-day gate lengths in transistors for commercial use can be of the order of  $0.1 \mu\text{m}$  in Si-based ones, and even as short as a few tens of nm in GaAs-based Shottky-gate and high-electron-mobility Field Effect Transistors (FET).

Such a miniaturization process poses several issues.

Even if less fundamental, one of these is that size reduction causes charge carriers to be driven by very intense electric field strengths, as high as several kV/cm, at ordinary voltages. It follows that electron transport takes place in a strongly nonlinear regime very far away from thermal equilibrium, where electrons can acquire energies of the order of several tenths of eV (hot electrons). Details of the conduction band therefore become relevant and a simple effective mass approximation is not applicable. A further complication stems from the circumstance that a number of phonon scattering mechanisms are active at room-temperature conditions, which are those of practical importance. Such a physical scenario prevents any realistic preliminary analysis of hot electron transport properties a necessary task for optimal device design to be performed through a solution of the Boltzmann equation.

Nanowires are filamentary crystals with diameters in the order of few nanometers. Thanks to their peculiar shape and dimensions, they are a great promise for many technological advances in this century in diverse areas such as biosensing, energy harvesting and optoelectronics . For the full deployment of such technology, control over the nanowire structure and composition at the nanometer scale is essential. In this frame, nanowire based heterostructures have been broadly studied .

A more fundamental consequence of miniaturization is that the increasing ability in building and controlling devices of nanometric size is going to cause a drastic change of the electron behavior due to the appearance of quantum effects. Indeed, although in most of the cases present-day microelectronic devices still have not reached such regime, semiconductor structures having one, two or even three

dimensions comparable with the electron wavelength and shorter than coherence length (nanostructures) are currently fabricated and investigated in many laboratories all over the world.

Study of transport in such nanostructures has a practical importance since it allows to gain knowledge on the behaviour of future devices where the wave-like behaviour of electrons is expected to cause the breaking of the Boltzmann equation picture. At the same time, such research activity is also relevant from the perspective of fundamental physics as it frequently occurs when first unattainable regimes become accessible allowing the discovery of new phenomena. At this purpose, semiconductors, and especially those of the family III-V such as GaAs, are particularly attractive since they exhibit quantum effects with relative ease due to the large electron wave and coherence lengths. This has led to the observation of striking phenomena such as the quantization of conductance, the quantum Hall effect and the fractional quantum Hall effect (the discoverers of the latter two were awarded the Nobel Prize in 1985 and 1998, respectively).

Such outstanding findings, and many others, have contributed in turn to give impetus to the search for innovative devices relying on coherent quantum behavior of conduction electrons, where the high and low conduction state are achieved through electrically controlled constructive and destructive interference, respectively.

An eminent paradigm among phase-coherent devices is the Datta-Das proposal for a novel spin-FET where coherent manipulation of electron spin is used for controlling conductance. Indeed, the study of transport in semiconductor devices where electron spin, instead of charge, degrees of freedom are exploited is receiving a growing attention up to the point that a whole research field called spintronics has emerged. Within this context, semiconductors once again prove to be particularly advantageous materials since their spin coherence times and lengths can respectively exceed 100 ns and 100  $\mu$  m. Such features also motivate the intense research activity aimed at using semiconductor nanostructures for quantum information processing devices. Electron spin is indeed one of the most promising proposals for encoding a qubit, the building block of the future quantum computer.

In the case of the 1D wire, we will demonstrate that control of electron transport through the manipulation of the quantum state of the magnetic impurities can be achieved by the singlet and triplet maximally entangled states. These have the property of respectively maximizing and minimizing electron transmission through the wire within the set of anti-aligned impurity spin states. Remarkably, such result suggests a novel use of quantum entanglement as a control resource of electron transmission through a 1D wire (entanglement-controlled transmittivity). We will find that even in the absence of a direct coupling between the impurities, the above maximally entangled states can be generated through electron scattering itself.

It is clear that the transport regimes involved in the MC study of bulk n-GaAs and in the investigation of transmission properties of quasi-1D structures are deeply different and, in a sense, almost “opposite”. Between two successive collisions, electrons behave as classical particles in the first case, and as waves in the case of quasi-1D structures (a fully quantum treatment being adopted in the latter case). In the bulk case, the condition of being at room temperature causes occurrence of phonon scattering, which is instead absent in the second case. The electric field is generally very intense in the first case and thus electron transport properties crucially depend on its strength while the linear response regime is analyzed in the second case and there is no dependence on the voltage intensity. Therefore, the present thesis consists in fact of two distinct parts. Yet, instead of presenting them in two separate sections, these are rather developed as long as possible along two parallel “tracks” in the introductory chapters. This is done with the hope to better highlight and thus appreciate the confinement effect, oscillator strength, optical properties, size effect and photoluminescence spectra of GaAs nanowire by partitioning the contents into chapters as follows: Introduction, the first chapter

,background of the study as the second chapter,the method of the study as third chapter ,result and discussion are organized under fourth chapter finally the remaining, conclusion,challenges,future outlook,application of GaAs nanowire are arranged under the last chapter.

In searching to discover semiconductor materials and metallic nanowire interconnect for new generation miniaturized electronic devices, nanostructures have been a focus of attention. Electronic devices, such as transistors based on carbon nanotubes, attracted interest in nanowires. Rodlike Si nanowires have been fabricated with a diameter of 1.3–7 nm. It has been shown that such Si nanowires can display metallic, semiconducting, and half-metallic properties depending on their functionalization. Being an alternative to silicon based microelectronics GaAs nanowire is one of the most important materials used in semiconductor physics. Due to the high electron mobility, GaAs always carried a potential of being used in high-speed electronic devices. GaAs/AlGaAs heterostructures have served as media for the two-dimensional electron-gas studies.

Similar to bulk crystals researcher have envisioned GaAs nanowires to be a potential alternative for Si nanowires. Recent advances in fabrication technology made it possible to grow GaAs nanowires. They are grown by metal catalysts in vapor-liquid-solid (VLS) mechanism. Generally, GaAs nanowires are grown along (111) direction in zinc-blende  $z\bar{6}$  structure, whereas nanowires with wurtzite  $w\bar{2}$  structure with diameter as small as 10 nm are also observed. Several models were developed to predict the transition radius from wurtzite to zinc-blende structure. Actually, there is no sharp transition but instead there are many different stacking configurations with very similar energies and more sophisticated models are needed to predict the ground-state configuration. Together with the crystal structure, surface face structure is also an important parameter affecting the structural and electronic properties.

The observation of visible photoluminescence( PL )in a variety of semiconductor nanocrystallites has fueled a large body of research work in the past decade. A material which has attracted considerable attention is porous gallium arsenide, which is a disordered collection of gallium arsenide nanocrystallites with varying sizes. The photoluminescence spectra from such systems are broad, and often asymmetric about the peak energy.

To compute the parameters of emission, or, equivalently, the spectral line shape from an ensemble of semiconductor nanowire, one needs to consider the distribution of crystallite sizes in the system. The luminescence depends on

1) the energy gap,

2)the oscillator strength, and

3) the exciton binding energy, among others. All these factors exhibit a dependence on the size of the nanowire. In this work, we provide a simple theoretical framework to calculate the spectral line shape,confinement effect ,energy gap,oscillator strength of GaAs nanowire from a existing optimal available literature, and illustrate the consequences of the result on earlier theoretical calculations and experimental analyses. We compare our results with the vast literature on light emission from gallium arsenide nanowire, and explain experimental observations on the basis of our model.

The light emission from silicon nanocrystallites at energies higher than the bulk Si gap was attributed by several workers to quantum confinement effects. The experimental validation of the quantum confinement model has been beset with difficulties, as several groups reported conflicting results. A case in point is the shift in the PL peak with varying crystallite size. Vial et al. and Schuppler et al. reported a distinct size dependence of the PL peak, though this was refuted by other groups based on their experimental works. Recently, an attempt was made to explain this conflict on the basis of a size distribution of nanocrystallites, based on a computer simulation study. Our model attempts to resolve the issues raised by these studies from GaAs nanowire point of view.

## 1.1 Energy quantization and band gap of gallium arsenide nanowire

A nanocrystal is a crystalline material with at list one dimension measured in nanometer scale. Nanoparticles are of great scientific interest as they are effectively a bridge between bulk materials and atomic or molecular structures. Bulk materials have size independent physical properties whereas nanomaterials show strong size dependence on their optical, electronic and thermodynamic properties. This is due to quantum confinement, hence quantum dots (QDs) very high surface area to volume ratio. One of the most important features of low-dimensional semiconductor structures is the confinement driven quantization of energy spectrum of charge carriers. The effect of quantum confinement becomes stronger as the confinement dimension increases and the size of a structure decreases. While bulk materials have a three-dimensional energy band structure, one-dimensional confinement of quantum wells leads to a two-dimensional energy band structure near each quantized energy level in the well and two-dimensional confinement of quantum wires leads to a one dimensional energy band structure near each quantized energy level in the wire. On the other hand, three-dimensional confinement in quantum dots lead to a discrete (atomic-like) lower part of the energy spectrum . The quantum confinement in different directions also changes wave functions describing the behavior of electrons and holes. As a result, the number of states per unit energy, the density of states, changes as a function of energy  $E$  of the particle shown in figure 1.

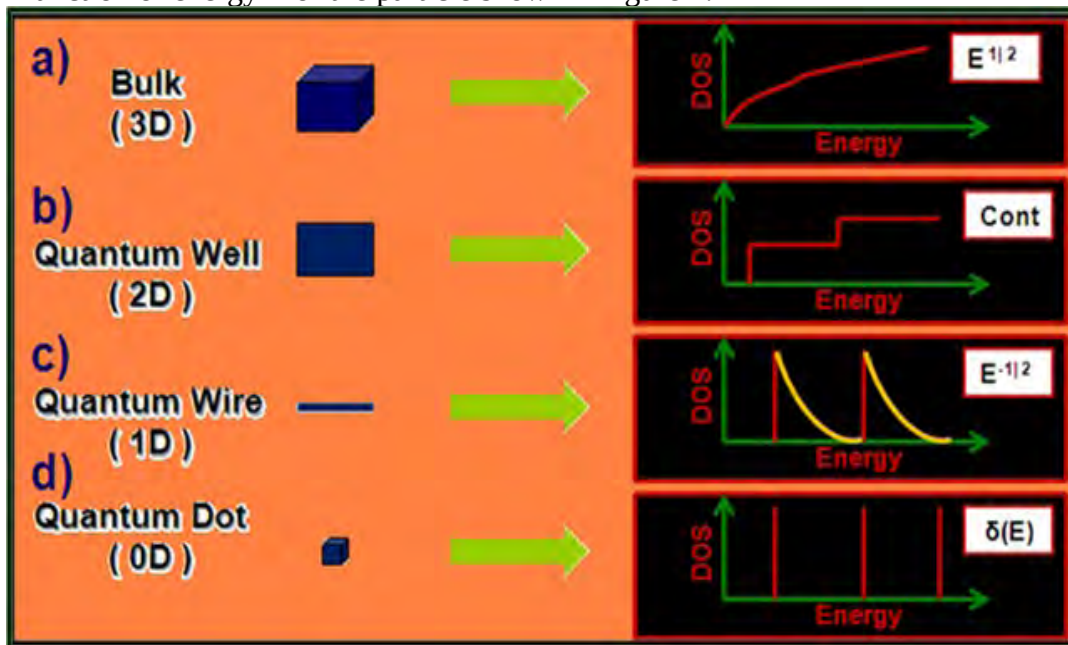


Figure 1. Electronic density of states of semiconductors with 3, 2, 1 and 0 degrees of freedom for electron propagation. 2, 1 and 0 degrees of freedom referred to as quantum wells, quantum wires and quantum dots respectively.

Generally the density of states depends on the dimension of the nano-structure and the corresponding wave vector dispersion relation. A particle behaves as if it were free when the confining dimension is large compared to the wavelength of the particle. During this state, band gap remains at its original energy due to continuous energy state. However, as the confining dimension decreases and reaches a certain limit, typically in nanoscale, the energy spectrum turns to discrete. As a result, band gap becomes size dependent. Specifically, the effect describes the phenomenon results from electrons and holes being squeeze into a dimension that approaches a critical quantum measurement, called the exciton Bohr radius.

In addition to the quantum confinement, lattice contractions and surface passivation can also alter the band-gap of a material. Several models have proposed in order to describe band structure of semiconductors. Among those different models, effective mass approximation (EMA) is the simplest model which describes the band-gap of nanostructures specially quantum dots. Hence, the simplest model of an infinitely strong confining potential (i.e. infinitely high potential barriers at the dot boundary) it is possible to estimate the energies of electrons and holes localized inside the nanocrystal as proportional to  $R^{-2}$ , where R is the nanocrystal radius.[1,17,14]

## ***1.2 Light emitting property of GaAs nanostructure***

GaAs is an important semiconductor with a direct gap (1.424eV) and a large exciton Bohr diameter (19nm). A great deal of interest has been generated in both the etching of GaAs and formation of an oxide layer on its surface due to their unique optical properties and various applications particularly in electronic devices and dry/wet solar cells. The rate and product of GaAs oxide depend on several factors; illumination, the PH of the electrolyte. The rate of these oxides increase by illumination because the carriers involved in oxide of GaAs are the valence bond holes. Working in strongly alkaline solutions prevents the growth of oxide layers but causes lattice dissolution, while working in neutral and acidic electrolytes favors oxide growth.

Lots of works have been done to research the photoluminescence property of porous GaAs. There are two basic assumptions of the origin of the visible photoluminescence in porous GaAs. The first explanation implies that the band in the visible region of photoluminescence is caused by residual products of the chemical reaction in the cause of etching. The second assumption associates visible photoluminescence with quantum confinement effects due to nano-sized GaAs crystallites. The average size of GaAs nano crystallites can be calculated from photoluminescence measurements.

Some very interesting photoluminescence properties have been observed. Porous GaAs produced in HF solution using p-type GaAs exhibits an infrared photoluminescence band and a yellow photoluminescence band. And porous GaAs fabricated in HCL solution using n-type GaAs shows an infrared photoluminescence band and the green photoluminescence band were explained by the quantum effect in nano-sized GaAs crystallites. However, there is no report about the relationship between the optical properties of electrochemical etched GaAs and etching temperature and the origin of green photoluminescence band is still not completely understood.

The microstructure and optical properties of anodized GaAs are discussed in detail by using micro-Raman and temperature dependence photoluminescence spectra.

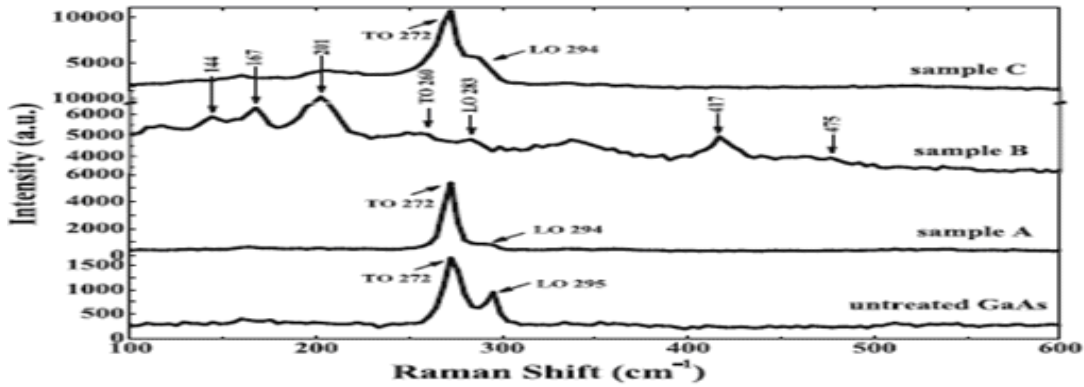


Figure 2. Raman spectra recorded at room temperature for different samples (A(at 3000 c),B(at 5000 c), C(at 7000 c))(adapted from 8)

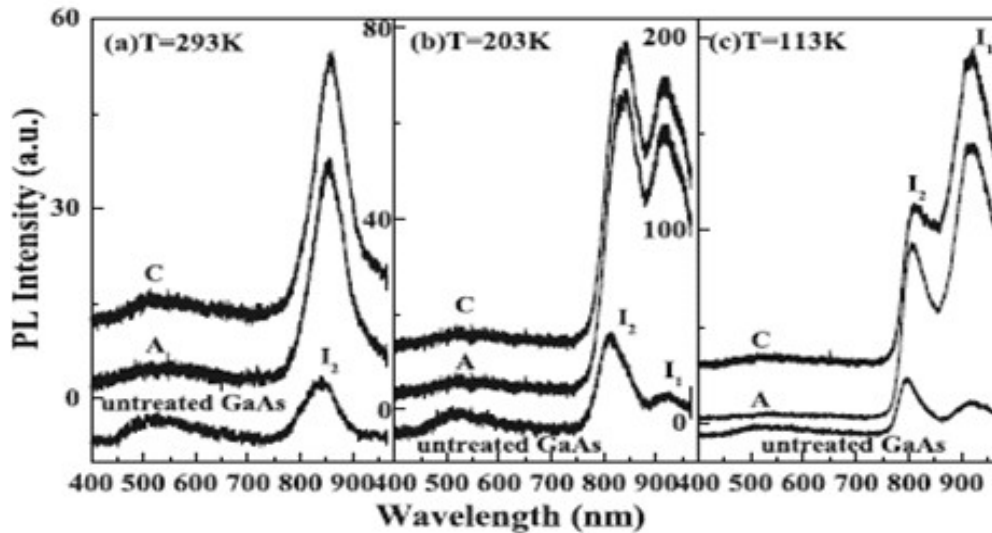


Figure 3. Temperature dependence photoluminescence spectra of untreated GaAs,sample A and C .

The broad and asymmetric raman peaks are observed in the anodized GaAs, which could be explained by phonon confinement effect. It is found that the GaAs granular films prepared at etching temperature of 5000 degree centigrade, reveals strongly enhanced visible photoluminescence, which could be [16] attributed to both the quantum confinement in GaAs nanocrystals and photoluminescence of oxides of gallium and arsenide. The estimation of the average diameter of GaAs nanocrystallites was made using the shift value of the Raman peak, the shift is due to longitudinal optical(LO) phonon of GaAs.

### 1.3 Oxide-assisted growth and optical characterization of gallium arsenide nanowires

Gallium arsenide GaAs as a direct-band-gap semiconductor with high electron mobility, has been widely used for the fabrication of laser diodes, full-color flat-panel displays, and high-speed transistors. Recently, the remarkable properties of one-dimensional nanostructures have stimulated intensive interest in the synthesis, characterization, and applications of GaAs nanowires. Several methods have been applied to synthesize GaAs nanowires, including laser assisted metal-catalytic growth, nanosize-pore template or mask growth, as well as sidewall growth based on electron-beam lithography. Recently, an oxide-assisted growth method has been developed to fabricate nanowires of silicon and germanium. This method not only produces nanowires in larger quantity than the prior methods, but it also requires no metal catalysts and/or templates as usually *needed in other methods*. Thus, it would *simplify the purification process and subsequent application of nanowires produced by this method*. As such, it is of interest to extend this method to the synthesis of binary or ternary compound semiconductor nanowires[1,2,7,9].

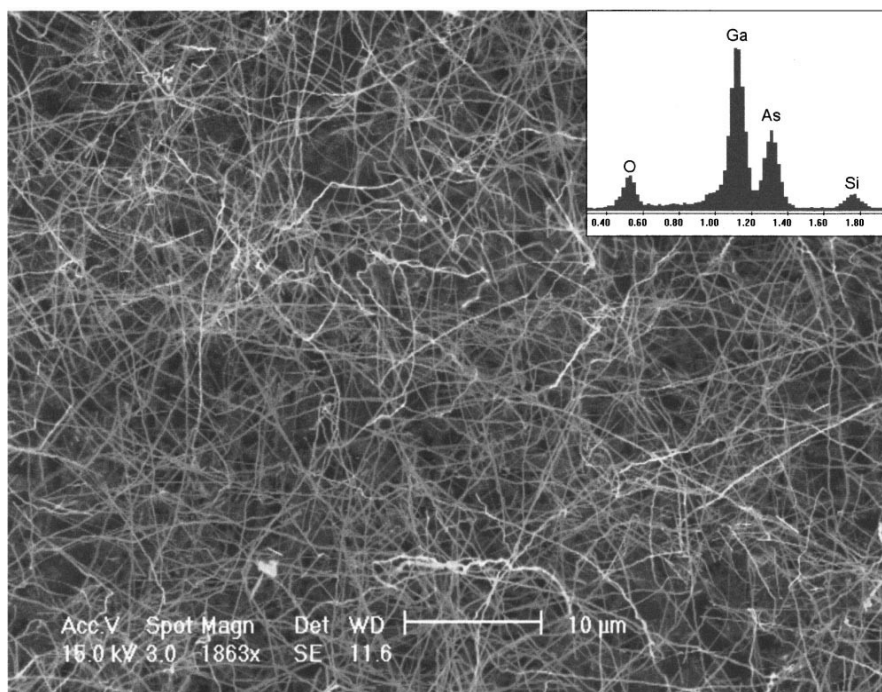


Figure 4. Typical SEM image of GaAs nanowires. Inset shows EDX spectrum taken from GaAs nanowires.

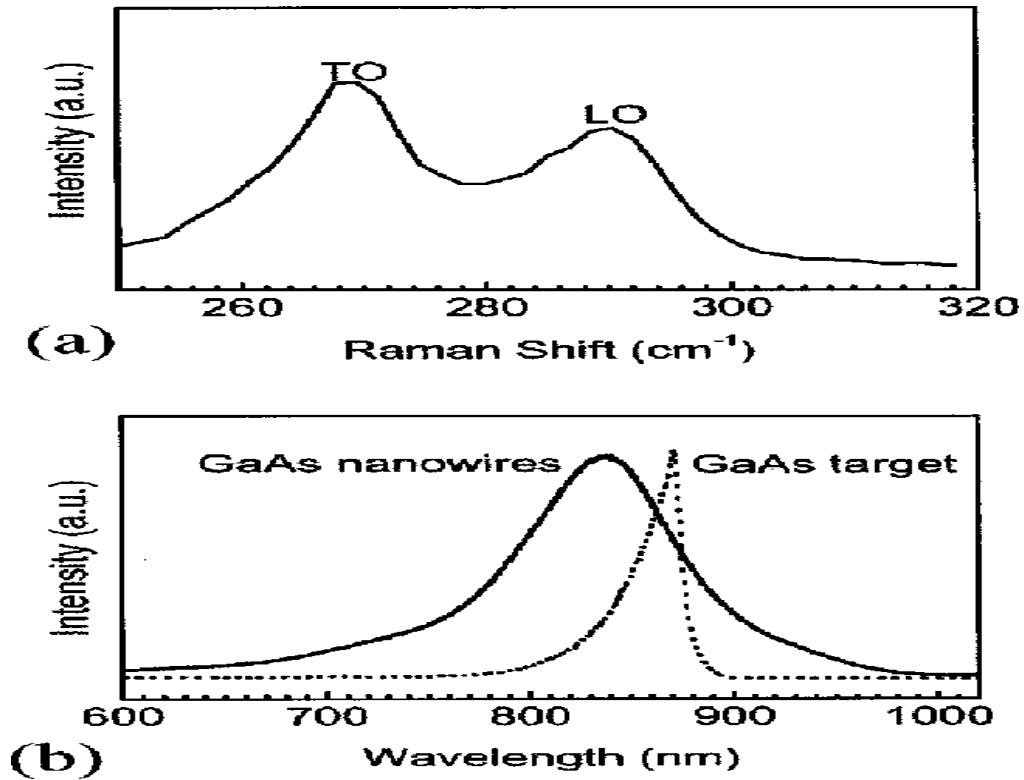


Figure.5 Room-temperature Raman spectrum (a) of GaAs nanowires and PL spectra (b) of GaAs nanowires and GaAs bulk crystal

In general to the above idea, GaAs nanowires were synthesized by the oxide-assisted method via the laser ablation of a mixture of GaAs and  $Ga_2O_3$ . Neither metal catalysts nor templates were used in this process. The length of the GaAs nanowires was up to tens of micrometers. The GaAs nanowire was composed of a crystalline core of 60 nm in diameter clothed by a thin amorphous-oxide layer with an average thickness of 5 nm. The growth was explained by a growth mechanism based on an oxidation-reduction reaction. Significant shifts and broadening were observed in the Raman and PL peaks, which were mainly attributed to stress, impurities, and defects in the GaAs nanowires.

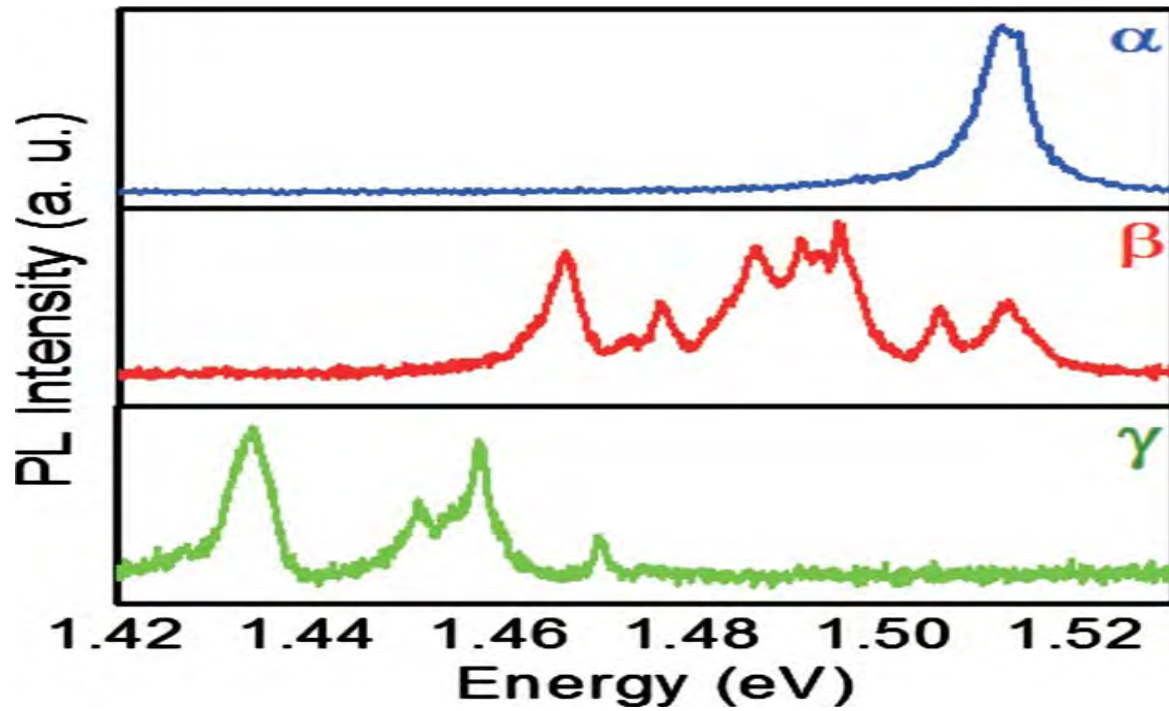


FIG. 6 Typical photoluminescence spectra observed from the three types of nanowires at  $T = 4.2$  K. The spectra have been obtained from single wires under illumination at 632.8 nm with a power density of  $2.5 \text{ W / cm}^2$ . The emission energy shifts from 1.51 eV down to 1.43 eV depending on the growth conditions which result in different proportion of wurtzite and zinc-blende GaAs.

## **1.4 Research Objectives**

The main interest of this research is to study the photoluminescence spectra of gallium arsenide nanowire and its confinement effect.

The objectives of this research can be summarized as the following:

- a) to study the electronic structures of gallium arsenide nanowire and the confinement effect with variable size and structures and comparing the energy gap.
- b) to study the relation between the bandgap and the structures size of the gallium arsenide nanowire.
- c) looking for optical properties, dielectric function, oscillator strength, complex refractive index, optical susceptibility .

## **1.5 Scopes of the Study**

*The scopes of this research are as the following*

- a) Nanowire is studied as isolated small range.
- b) Gallium arsenide nanowire is adopted as the material of the study.
- c) Band structures, quantum confinement and energy spectrum are studied for the electronic structures of gallium arsenide nanowire .
- d) Effective mass approximation is used to calculate the bandgap of gallium arsenide nanowire.

# Chapter 2

## 2. Bulk and nanostructured semiconductor systems

As this work is concerned with transport in semiconductor materials, in this chapter we provide a description of the features of such systems both bulk and nanostructured which are of relevance for the phenomena to be investigated in this study.

Although transport of charge in semiconductors can take place through both electrons and holes, throughout this thesis we will deal with n-type semiconductors and we are thus concerned with transport of electrons. As a consequence, we shall predominantly focus only on the conduction band since the valence band does not play any essential role in the physical phenomena under study.

After a short recall of the general properties of semiconductors, we shall illustrate the main features of gallium arsenide (GaAs) nanowire such as the conduction band structure and all the relevant electron scattering processes. From one hand, our focusing is on GaAs nanowire. [4]

This compound has its own importance since it is nowadays one of the most widely used and studied semiconductors. On the other hand, GaAs nanowire can be regarded as a significant paradigm given that many of the concepts and topics which will be introduced referring to this material (such as the effective mass approximation, the three-valley model, the nonparabolicity effects and many electron scattering processes) are generally valid for any semiconductor and in particular for the III-V semiconductors. Furthermore, GaAs is at present the most used material in the growth of semiconductor nanostructures due to its superior ability of exhibiting quantum effects compared to Si.

An introduction to semiconductor nanostructures is given together with a description of a paradigmatic example, namely the GaAs nanowire as heterostructure. Basic concepts such as optical properties, dielectric function, oscillator strength and quantum confinement and energy gap of such systems and subbands are then analyzed. It follows a description of structures of particular interest such as quantum wells, quantum wires and quantum dots.

Therefore after introducing semiconductor, we will briefly discuss the background of gallium arsenide and its band gap. Finally discussing effective mass approximation, namely the most common way of modeling the conduction band of semiconductors. At the end of this chapter we show how quantum effects arising from confinement of one or more degrees of freedom result in a splitting of the energy band structure into subbands. But also the chapter is devoted to nanostructures where at least one degree of freedom is unconstrained, namely quantum wells and quantum wires. Finally, we discuss quantum dots which are structures where all the three degrees of freedom are confined.

### 2.1 Semiconductors

Low-dimensional GaAs structures, such as quantum wires and the quantum dots, attract attention in recent years as objects for basic research, and as perspective materials for fabrication of new devices that cannot be fabricated from crystalline semiconducting materials.

As suggested by their name, semiconductors have electric conduction properties intermediate between those of insulators and metals. Indeed, while typical room temperature resistivities in metals and good insulators are around  $10^{-6}$  and  $10^{12}$   $\Omega$  cm, respectively, being able to reach even the value of  $10^{22}$   $\Omega$ cm in the latter case, in semiconductors they usually fall in the range  $10^{-3}$  to  $10^9$   $\Omega$ cm.

This classification scheme is however quite unsuitable as a criterion for assessing whether a solid is a semiconductor or not since it hides those crucial physical features which significantly distinguish semiconductors from insulators and, above all, from metals. [14]

Among these, the most outstanding one is maybe the so called negative temperature coefficient of resistance, namely the existence of a temperature range below the melting point where, unlike metals, the electrical resistance falls as the temperature is raised. The discovery of this phenomenon in silver sulphide by Faraday in 1834 is commonly regarded as the starting point of semiconductor physics. Other peculiar phenomena typically exhibited in semiconductors are: high values of thermopower of both signs, photo-conductivity and photo-voltaic effect (both first observed in selenium in 1873 by Smith and in 1876 by Adams and Day, respectively), rectification (first noticed by Braun in 1874) and more in general non-ohmic behaviors, evidence for positive charge carriers through Hall effect measurements.

Quantum theory of solids, mainly through the work of Bloch and Wilson, has led to a satisfactory explanation of such phenomena providing at the same time a valid criterion for characterizing semiconductors. This can be accomplished in terms of the energy gap  $E_g$  between the bottom of the conduction band and the top of the valence band. A solid is said a semiconductor if all its electron bands are completely empty or filled at temperature  $T = 0$  K, but  $E_g$  is narrow enough to allow an observable conductivity to be exhibited at temperatures below the melting point, such conductivity being due to thermal excitation of electrons into the conduction band. In most important semiconductors  $E_g < 2$  eV.

The key ingredient for the great success and wide use of semiconductors – not only from the mere technological perspective – is the relatively low and variable number of charge carriers compared to metals. Such features can be fruitfully used to control conductivity and explain why electrical conduction of semiconductors is highly sensitive to the presence of substitutional impurity atoms or, in short, impurities.

These can be of two kinds: donors and acceptors. An atom of the pure material is replaced by an impurity atom with a larger number of valence electrons in the first case and with a lower number in the second case. A donor atom donates weakly-bound valence electrons (not involved in covalent bonds) to the conduction band, creating excess negative charge carriers. The opposite behaviour occurs for an acceptor atom which is able to accept as many electrons from the valence band as many are needed to reach the valence of the substituted atom. The accepted electrons leave unoccupied levels in the valence band, namely holes, creating excess positive charge carriers. A semiconductor doped with donor (acceptor) impurities is said of n-type (p-type) and its chemical symbol is commonly written with the prefix “n-” (“p-”). The number of donated charge carriers usually far exceeds the very small number of the intrinsic ones. It follows that in an n-type (p-type) material, provided the doping level is not too low (typically an impurity concentration of 1 p.p.m. is enough), only electrons (holes) in fact contribute to electrical conduction, with the density of these carriers being equal to the concentration of dopants (if one electron/hole is donated by each impurity). This implies the ability of setting the carrier concentration in such materials since n-type and p-type semiconductors can be grown with a desired doping level.[5]

## 2.2. SEMICONDUCTING NANOPARTICLES

### *Optical Properties*

Because of their role in quantum dots, nanoparticles made of the elements, which are normal constituents of semiconductors, have been the subject of much study, with particular emphasis on their electronic properties. The title of this section, “semi-conducting nanoparticles,” is somewhat misleading. Nanoparticles made of cadmium, germanium, or silicon are not themselves semiconductors. A nanoparticle of Si, can be made by laser evaporation of a Si substrate in the region of a helium gas pulse. The beam of neutral clusters is photolyzed by a UV laser producing ionized clusters whose mass to charge ratio is then measured in a mass spectrometer.[3]

The most striking property of nanoparticles made of semi-conducting elements is the pronounced changes in their optical properties compared to those of the bulk material. There is a significant shift in the optical absorption spectra toward the blue (shorter wavelength) as the particle size is reduced.

In a bulk semiconductor a bound electron-hole pair, called an exciton, can be produced by a photon having an energy greater than that of the band gap of the material. The band gap is the energy separation between the top filled energy level of the valence band and the nearest unfilled level in the conduction band above it. The photon excites an electron from the filled band to the unfilled band above. The result is a hole in the otherwise filled valence band, which corresponds to an electron with an effective positive charge. Because of the Coulomb attraction between the positive hole and the negative electron, a bound pair, called an exciton, is formed that can move through the lattice. The separation between the hole and the electron is many lattice parameters. The existence of the exciton has a strong influence on the electronic properties of the semiconductor and its optical absorption. The exciton can be modeled as a hydrogen-like atom and has energy levels with relative spacings analogous to the energy levels of the hydrogen atom but with lower actual energies.

Light-induced transitions between these hydrogen like energy levels produce a series of optical absorptions that can be labeled by the principal quantum numbers of the hydrogen energy levels. We are particularly interested in what happens when the size of the nanoparticle becomes smaller than or comparable to the radius of the orbit of the electron-hole pair. There are two situations, called the weak-confinement and the strong-confinement regimes. In the weak regime the particle radius is larger than the radius of the electron-hole pair, but the range of motion of the exciton is limited, which causes a blue shift of the absorption spectrum. When the radius of the particle is smaller than the orbital radius of the electron hole pair, the motion of the electron and the hole become independent, and the exciton does not exist. The hole and the electron have their own set of energy levels. Here there is also a blue shift, and the emergence of a new set of absorption lines .

## 2.3 Energy Bands and Gaps of Semiconductors

The electrical, optical, and other properties of semiconductors depend strongly on how the energy of the delocalized electrons involves the wave vector  $k$  in reciprocal or  $k$  space, with the electron momentum  $p$  given by  $p = \hbar k$ . We will consider three-dimensional crystals, and in particular we are interested in the properties of the (3&5 group) and group 2 semiconducting compounds, which have a cubic structure, so their three lattice constants are the same:  $a = b = c$ .

The electron motion expressed in the coordinates  $K_x, K_y, K_z$  of reciprocal space takes place in the Brillouin zone, and the shape of this zone-for these cubic compounds is shown in figure . Points of high symmetry in the Brillouin zone are designated by capital Greek or Roman letters, as indicated.

The energy bands depend on the position in the Brillouin zone, and Figure presents these bands for the intrinsic (i.e., undoped) 3&5 group compound GaAs. The

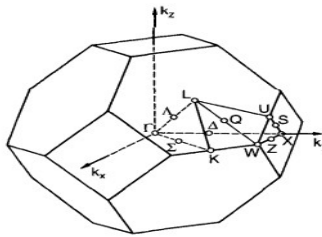


**Figure 2.14.** Brillouin zone of the gallium arsenide and zinc blende semiconductors showing the high-symmetry points  $\Gamma$ ,  $K$ ,  $L$ ,  $U$ ,  $W$ , and  $X$  and the high-symmetry lines  $A$ ,  $A'$ ,  $Z$ ,  $Q$ ,  $S$ , and  $Z'$ . (From G. Burns, *Solid State Physics*, Academic Press, Boston, 1985, p. 302.)

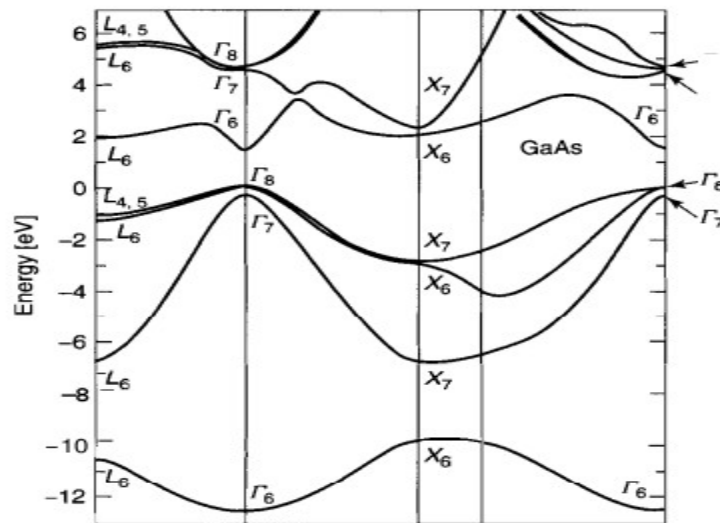


**Figure 2.15.** Band structure of the semiconductor GaAs calculated by the pseudopotential method. (From M. L. Cohen and J. Chelikowsky, *Electronic Structure and Electronic Properties of Semiconductors*, 2nd ed., Springer-Verlag; *Solid State Sci.* 75, Springer, Berlin, 1989.)

figure plots energy versus the wavevector  $k$  in the following Brillouin zone directions: along A from point  $r$  to X, along A from to L, along C from  $r$  to K, and along the path between points X and K. These points and paths are indicated in the sketch of the Brillouin zone in Fig. 2.14. We see from Fig. 2.15 that the various bands have prominent maxima and minima at the central point  $r$  of the Brillouin zone. The energy gap or region where no band appears extends from the zero of energy at point  $T_s$  to the point  $r$  directly above the gap at the energy  $E_g = 1.35\text{eV}$ . The bands below point  $\Gamma_8$  constitute the valence band, and those above point  $\Gamma_6$  form the conduction band. Hence  $T_s$  is the lowest energy point of the conduction band, and  $\Gamma_8$  is the highest point of the valence band.

At absolute zero all the energy bands below the gap are filled with electrons, and all the bands above the gap are empty, so at absolute temperature 0 K the material is an insulator. At room temperature the gap is sufficiently small so that some electrons are thermally excited from the valence band to the conduction band, and these relatively few excited electrons gather in the region of the conduction band immediately above its minimum at  $\Gamma_6$ , a region that is referred to as a “valley.” [18]

These electrons carry some electric current, hence the material is a semiconductor.

Gallium arsenide is called a direct-bandgap semiconductor because the top of the valence band and the bottom of the conduction band are both at the same center point ( $r$ ) in the Brillouin zone, as is clear from Fig. 2.15. Electrons in the valence band at point  $\Gamma_8$  can become thermally excited to point  $r$  in the conduction band with no change in the wave vector  $k$ .

The compounds GaAs, GaSb, InP, InAs, and InSb and all the III-V compounds included in have direct gaps. In some semiconductors such as Si and Ge the top of the valence band is at a position in the Brillouin zone different from that for the bottom of the conduction band, and these are called indirect-gap semiconductors.

## 2.4 ELECTRON TRANSPORT IN DIRECT GAP SEMICONDUCTORS: Gallium Arsenide(GaAs)

Gallium arsenide (GaAs) belongs to the family of the so called semiconductor compounds III-V. These are nine binary compounds resulting from the combination of In, Ga, Al (elements from column III of the periodic table) with Sb, As, P (elements from column V).

They typically consist of crystals of the zincblende structure with a bonding generally having both an ionic and a covalent fraction (in GaAs the bonding is exactly half ionic and half covalent). Doping of GaAs is usually performed using Si atoms (group IV) as substitutional impurities obtaining n-GaAs when Si replaces Ga and p-GaAs when Si replaces As. A typical impurity concentration is of the order of  $10^{15}\text{ cm}^{-3}$  to be compared with the number of atoms per unit volume of intrinsic GaAs which is  $4.42 \times 10^{22}\text{ cm}^{-3}$ .

The use of GaAs for practical applications – especially those for which it is preferred to Si – mainly relies on properties such as its **high saturated electron velocity and electron mobility, low noise at high frequencies, high breakdown electric field and direct band gap.**

GaAs is used in infrared light-emitting diodes, laser diodes, photodetectors, solar cells, mobile phones, satellite communications, radar systems. For some time in the 1980's it was believed that Si-based microelectronics was going to be replaced by a GaAs-based one (the attempts done proved eventually unsuccessful), this expectation being motivated by the attractive high switching speed of gallium arsenide devices. Moreover, GaAs is of great importance for quantum nanostructures due to its ability **in exhibiting quantum effects with relative ease**, this being largely due to its **low electron effective mass**. [11]

Determining the energy band structure of a semiconductor is far from being a trivial task and in general requires quite sophisticated computational techniques. In the case of GaAs, a lot of work has been carried out, mainly motivated by the several applications of this material, and the band structure of gallium arsenide nanowire is now quite well established.

## 2.5 QUANTUM WELLS, WIRES, AND DOTS

When the size or dimension of a material is continuously reduced from a large or macroscopic size, such as a meter or a centimeter, to a very small size, the properties remain the same at first, then small changes begin to occur, until finally when the size drops below 100 nm, dramatic changes in properties can occur. If one dimension is reduced to the nanorange while the other two dimensions remain large, then we obtain a structure known as a quantum well. If two dimensions are so reduced and one remains large, the resulting structure is referred to as a quantum wire. The extreme case of this process of size reduction in which all three dimensions reach the low nanometer range is called a quantum dot. The word quantum is associated with these three types of nanostructures because the changes in properties arise from the quantum-mechanical nature of physics in the domain of the ultrasmall.

## 2.6 PREPARATION OF QUANTUM NANOSTRUCTURES

One approach to the preparation of a nanostructure, called the bottom-up approach, is to collect, consolidate, and fashion individual atoms and molecules into the structure. This is comed out by a sequence of chemical reactions controlled by catalysts. It is a process that is widespread in biology where, for example, catalysts called enzymes assemble amino acids to construct living tissue that forms and supports the organs of the body.

The opposite approach to the preparation of nanostructures is called the top-down method, which starts with a large-scale object or pattern and gradually reduces its dimension or dimensions. This can be accomplished by a technique called Lithography which shines radiation through a template on to a surface coated with a radiation-sensitive resist; the resist is then removed and the surface is chemically *treated to produce the nanostructure*. [20]

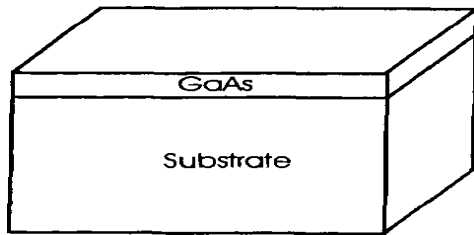


Figure 7a

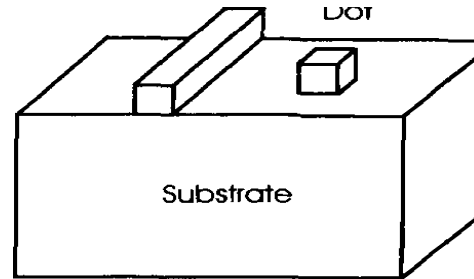


Figure 7b

a) Gallium arsenide quantum well on a substrate; (b) quantum wire and quantum dot formed by lithography.

The lithographic process is illustrated by starting with a square quantum well located on a substrate, as shown in Fig7. The final product to be produced from the material (e.g., GaAs) of the quantum well is either a *quantum wire* or a *quantum dot*, as shown in Fig. 7

## 2.6.1 Quantum Dots

Quantum dots (QDs) are nanometer scale "boxes" for selectively holding or releasing electrons. They are small physical devices that contain a "tiny droplet" of free electrons, small metal or semiconductor boxes that hold a specified number of electrons (Qds generally look more like pyramids than actual dots). QDs are grouping of atoms so small that the addition or removal of an electron will change its properties in a significant way. QDs are semiconductor structures where the electron wave function is confined in all three dimensions by the potential energy barriers that form the QDs boundaries. Specifically, QDs are semiconductor structures that confine the electrons and holes to a volume of order of  $20\text{nm}^3$ .

Modern semiconductor processing techniques permit the artificial creation of quantum confinement (quantum confinement in all three spatial dimensions) of only few electrons; such a finite fermions QD systems have much in common with the atoms, yet they are man made structures, designed and fabricated in the laboratory. The fabrication of Qds in semiconductor devices has led to the invention of a single electron transistors and controllable single-photon emitters. [19]

The generalization of the Schrodinger equation in three dimension is:

$$-\frac{\hbar^2}{2m}\nabla^2\Psi(r) + U(r)\Psi(r) = E\Psi(r)$$

The solution of the differential equation(1)for a particle in 3D infinite trap of volume with impermeable walls are given as:

$$\Psi_n(x, y, z) = \left(\frac{2}{L}\right)^{\frac{3}{2}} \sin\left(\frac{n_x\pi x}{L}\right) \sin\left(\frac{n_y\pi y}{L}\right) \sin\left(\frac{n_z\pi z}{L}\right)$$

and the corresponding energy eigen value will be

$$E_n(x, y, z) = \frac{\hbar^2 \pi^2}{2mL^2}(n_x^2 + n_y^2 + n_z^2)$$

A”hole”(missing electron)in a full energy band behaves very much like an electron except that it has a positive charge,and tends to float to the top of the band, i.e the energy of the hole increases oppositely to the energy of an electron The rules for nanonphysics that have been developed so far are also applicable for holes in semiconductors. To create an electron hole pair in semiconductors requires energy at least equal to the energy band gap  $E_g$  of the semiconductor .

## 2.6.2 Quantum wires (nanowires)

Nanowires (also called quantum wires) are 1D molecular structure with electrical and/or optical properties. Nanowires are examples of nanostructures, have attracted extensive interest in recent years because of their unusual quantum properties and potential use as nanoconnectors and nanoscale devices. In order to have enhanced physical properties, the wires must be of small diameter, must have high aspect ratio (i.e. the ratio length to thickness), and must be uniformly oriented. Nanowires are relatively easy to produce and can have different shapes. They are often thin and short ”threads” but can also have other manifestations. Gallium arsenide quantum wires have been produced (these are referred to as GaAs/AlGaAs quantum wires). Nano wires are being considered for use in the next generation computer chips. The propagation of electromagnetic energy has been demonstrated along a noble metal stripes with band of a few microns; propagation has also been demonstrated along nanowires with sub wave length cross sections and propagation length of a few micron. Metal nanowires can also be used to ”transmit” photons. The optical properties of metal nanowires can be optimized for particular wave length of interest, and non-regular cross-sections and coupling between closely spaced nanowires allows a tunneling of optical response. [1]

The term quantum wire describes a carrier confined in two dimensions say Y and Z to a small dimension d(wire cross-section d) and free to move along the length of the wire X(qualitatively this situation resembles the situation of the carrier moving along a carbon nanotube, or silicon nanowire, although the details of the bound state wave functions are different)

In the case of quantum wire of a square cross-section

$$\Psi_{mn}(x, y, z) = \left(\frac{2}{d}\right) \sin\left(\frac{n_y y}{d}\right) \left(\sin\left(\frac{n_z z}{d}\right)\right) \exp(iK_x X)$$

and the corresponding energy is

$$E_n(x, y, z) = \frac{\hbar^2 \pi^2}{2md^2} (n_x^2 + n_y^2) + \frac{\hbar^2 K_x^2}{2m}$$

### 2.6.3 Quantum Wells

A physical situation that often arises in semiconductor devices is a carrier confined in one dimension, say Z to a thickness d and free in two dimensions say X and Y this is called *2D bands or quantum wells*. *In this case the solution of the schrodinger equation will have the form*

$$\Psi_n(x, y, z) = \left(\frac{2}{d}\right)^{\frac{1}{2}} \sin \frac{n_z \pi z}{d} \exp(ik_x x) \exp(ik_y y)$$

and the energy of the carrier in the  $n^{th}$  band[1-2] is

$$E_n = \frac{\hbar^2}{2md^2} n_z^2 + \frac{\hbar^2 k_x^2}{2m} + \frac{\hbar^2 k_y^2}{2m}$$

## 2.7 Photoluminescence

Electrons are excited across the band gap, from the valence band to the conduction band, by providing an appropriate energy greater than the band gap of the material. These excited electrons must decay back to the valence band by radiative or non-radiative thermal process. Non-radiative processes are predominant routes to de-excitation when the electron-phonon coupling is strong. Phonon coupling provides quasi-continuous states which the electrons can occupy successively to de-excite to the ground state. In the absence of strong phonon coupling, the electrons have to make a radiative transition that often corresponds to energies close to the visible region of the electromagnetic spectrum. This phenomenon, known as photoluminescence. [15]

Photoluminescence can occur in nanocrystals in a variety of ways; for example, the electron-hole recombination can take place by involving the electronic states at the band edge, surface, defect and other trap states, or states on doped impurity atoms, giving rise to photoluminescence at different energies for the same material.

Electrons can de-excite radiatively by a transition from the bottom of the conduction band to the top of the valence band. In the absence of any significant trap states, the energy absorbed by the system to create an electron-hole pair will necessarily be equal to the energy emitted, when the electron and the hole recombine without the loss of any energy prior to the emission. The presence of unquenched dangling orbitals at the surface or any defect states in the bulk, provide traps for the excited electrons and the holes prior to their recombination. These orbitals have their energies in the band gap regions. Therefore, an electron excited to the conduction band can transfer itself non-radiatively to one of these surface or defect states before making a radiative transition to a lower energy state, likewise, a hole excited in the valence band can move into the defect states depending upon the donor/acceptor character of the defect states. The net result of such non-radiative transfers of electrons and holes to lower energy states prior to radiative recombination is that the emission occurs at energies much lower than the band gap energy of the nanocrystals, in contrast to the band edge recombination considered earlier. This is often referred to as the red shifted emission in nanocrystals.

## CHAPTER THREE

### METHODS OF THE STUDY

In this paper we present a detailed analysis of the atomic and electronic structures of GaAs nanowires using first-principles pseudo-potential calculations and considering existing experimental data to investigate the photoluminescence spectra of gallium arsenide with different types of nanowires with different diameters all grown along  $111\bar{2}$  direction, and we reveal interesting trends about their size, oscillator strength, optical property by using effective mass approximation and as core method we use curve fitting model by matlab program to compare our work with existing data and its validity. Finally by plotting the graph, and apply curve fitting model. These nanowires become semiconducting upon hydrogen passivation. Even if the band gap of some nanowires decreases with increasing diameter and hence reveals the quantum confinement effect, generally the band-gap variation is rather complex, and depends on the type and geometry, diameter, type of relaxation, and also whether the dangling bonds of surface atoms are saturated with hydrogen.[13]

#### 3.1 Effective mass approximation

The knowledge of the electron energy band structure  $\epsilon_c(k)$  is an essential requirement for the study of transport properties of a semiconductor. However, as it can be argued for instance in the case of GaAs the form of  $\epsilon_c(k)$  is usually complex and thus quite difficult to be accounted for. Fortunately, as it typically occurs in physics, we can fruitfully use some approximations.

The most well-known approximation of a semiconductor band structure is the so called effective mass approximation. Unlike metals, one can expect that due to the relatively small carrier density of a semiconductor only the lowest part of the conduction band  $\epsilon_c(k)$  is significantly occupied, namely those states near the lowest minimum (minima).

A frequently encountered case is when the absolute minimum of the conduction band lies at the center of the first Brillouin zone (that is at the wave vector  $k = 0$ ) as for GaAs.

The idea is thus to approximate  $\epsilon_c(k)$  with its second-order series expansion around the  $\Gamma$  point (from now on we omit the index  $c$  since we shall be always concerned with the conduction band).

This yields

$$\epsilon(k) = \epsilon_0 + Ak_x^2 + Bk_y^2 + Ck_z^2 \dots\dots\dots(1)$$

where  $\epsilon_0$  stands for the minimum of the conduction band and where  $A$ ,  $B$  and  $C$  are positive coefficients. In the case of a crystal with cubic symmetry (as GaAs), the above coefficients turn out to be equal and setting  $\epsilon_0$  to zero equation above can be put in the form[5] of this if  $A=B=C$ ,

$$E = \frac{\hbar^2 k^2}{2m^*}$$

The first derivative of this expression provides the velocity  $v$

$$\frac{1}{\hbar} \frac{dE}{dk} = v$$

and the second derivative provides the effective mass  $m^*$

$$\frac{1}{\hbar^2} \frac{d^2E}{dk^2} = \frac{1}{m^*}$$

For a semiconductor the electron is in the conduction band, and the hole is in the valence band. The electron and hole both have effective masses  $m_e$  and  $m_h$ , respectively, which are less than that of the free electron, so the effective mass is given by

$$m^* = m_e m_h / (m_e + m_h)$$

$$m^* = \frac{m_e}{1 + (m_e/m_h)}$$

## CHAPTER FOUR

### RESULTS AND DISCUSSION

We now examine the size dependencies of individual properties in detail. The variation of the oscillator strength ( $f_{osc}$ ) with the crystallite diameter  $d$  is usually assumed to be of a polynomial form such as

$$f_{osc} = d^{-\beta} \dots\dots\dots 1$$

by effective-mass-theory (EMT)-based calculations. Hybertsen and Needels as well as Khurgin et al. suggested  $\beta = 6$ , whereas Sanders and Chang proposed a value of 5. Local-density-approximation-based calculations on gallium arsenide clusters, however, showed a non-monotonic variation of the oscillator strength with crystallite diameter.

Within a simple effective-mass theory, the energy up-shift due to quantum confinement can be expressed as

$$\Delta E = \frac{C}{d^x} \dots\dots\dots 2$$

where  $x=2$ . However, both ab initio as well as semi empirical electronic structure calculations on silicon clusters suggest values of  $x$  in the range 1.4–2.

The exciton binding energy in semiconductor nanocrystallites is of a much smaller magnitude than the emission energy. Consequently, the effect of its size dependence on the spectral line shape is small. Factors such as the presence of non-radiative centers on the crystallite surface also affect photoluminescence, but theoretical calculations indicate that

- 1) even the presence of a single non-radiative center can kill luminescence in a nanocrystallite; and
- 2) given the small surface area, the probability of there being a non-radiative center is small, as indicated by the high luminescence efficiency. To preserve the simplicity of the model and bring out the essential physics in the system, we focus on the oscillator strength and the energy gap.

To compute a general expression for the PL spectrum, we assume a Gaussian size distribution for the nanocrystallites,

$$p(d) \approx \exp\left[-\frac{(d-d_0)^2}{2\sigma^2}\right] \dots\dots\dots 3$$

where  $d_0$  is the mean crystallite diameter and  $\sigma$  the variance of the crystallite size distribution.

$$I(\Delta E) = \int I(d) n(d) \delta(\Delta E - \frac{\beta}{d^\gamma}) d d$$

taking

$$n(d) = \frac{1}{\sigma\sqrt{2\pi}} \exp(-\frac{(d - d_0)^2}{2\sigma^2})$$

So, we obtained an expression for the photoluminescence intensity as

$$I(\Delta E) \sim \frac{1}{\sigma\sqrt{2\pi}} \left(\frac{\beta}{\Delta E}\right)^{\frac{2}{\gamma}} \exp\left[-\frac{\left\{\left(\frac{\beta}{\Delta E}\right)^{\frac{1}{\gamma}} - d_0\right\}^2}{2\sigma^2}\right]$$

It is clear from the above expression is that the photoluminescence intensity depends strongly on the quantum confinement parameters  $\beta$  and  $\gamma$ .

The number of atoms participating in the radiative process is proportional to the volume of the crystallite.

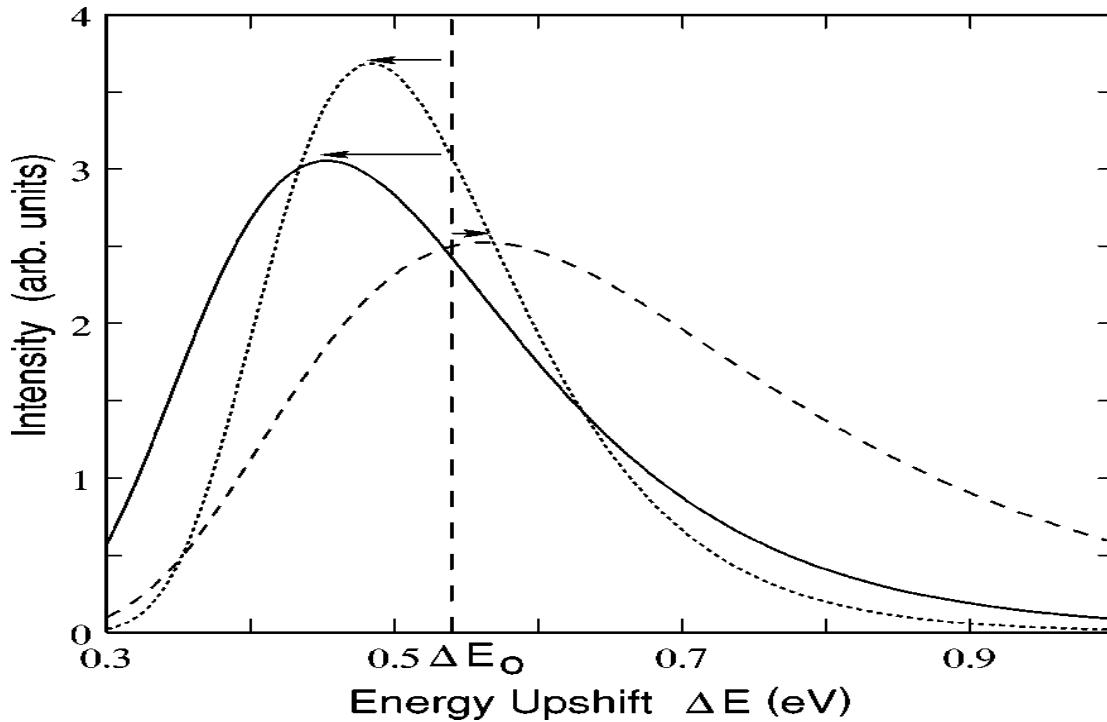


Figure 8. Theoretical PL spectra based on the above equation , The solid line depicts the case when  $k=5$ ( i.e.,  $m=2$ ,  $x=2$ , and  $\beta = 0$ ). The broken line is plotted with  $m=2$ ,  $x=2$ , and  $\beta =6$  ( $k=-1$ ), and shows a blue shift. The dotted line corresponds to  $m=2$ ,  $x=1.4$ , and  $\beta =0$ . The plots are normalized, with  $c=485.816$  eV/Å<sup>2</sup>.

Hence we can write the probability of emission from a nanocrystallite of diameter  $d$  as

$$P_r(d) = KV(d) f_{osc}(d) p(d) = Kd^m \frac{1}{d^\beta} \exp\left[-\frac{(d-d_0)^2}{2\sigma^2}\right] \dots\dots\dots 4$$

where  $K$  is an appropriate normalization constant, and  $m=2$  for columnar crystallites and  $m=3$  for nearly crystallites .Transforming the above expression to the energy axis, we obtain

$$\left. \begin{aligned} P(\Delta E) &= K \int_0^\infty \delta\left(\Delta E - \frac{c}{d^x}\right) d^m \frac{1}{d^\beta} \exp\left[-\frac{(d-d_0)^2}{2\sigma^2}\right] d(d) \\ &= N \Delta E^{-k/x} \exp\left[-\frac{\alpha^2}{2} \left\{\left(\frac{\Delta E_0}{\Delta E}\right)^{1/x} - 1\right\}^2\right], \end{aligned} \right\} \dots\dots\dots 5$$

where  $N$  is a normalization constant, and we have defined

$$\left. \begin{aligned} \Delta E_0 &= \frac{c}{d_0^x} \\ k &= m - \beta + x + 1 \\ \alpha &= \frac{d_0}{\sigma} \end{aligned} \right\} \dots\dots\dots 6$$

In Figure. 8, we depict theoretical spectra based on the above equation. The values assigned to.  $c$  was chosen to be  $485.816$  eV/ Å<sup>2</sup> based on the work of Read et al.<sup>17</sup> Most of the experiments on porous silicon report the crystallite sizes to be in the range 20–40 Å. We have chose our mean crystallite size to be 30 Å, and assumed  $\sigma = 3A^0$  . The solid line ( $m=2, x=2$ ) and the dotted line ( $m=2, x =1.4$ ) are for the case  $\beta = 0$  . The broken line depicts the when  $m=2, x=2$ , and  $\beta = 6$  . We see that the peak

positions in both cases are substantially different. This raises question about the assignment of the exciton binding energy which was discussed in an earlier work. We shall discuss this issue later in this paper.

Most experiment report a variation of the luminescence peak with experimental parameters. The PL peak position  $\Delta E_p$  is given by the maxima in Equation above ,

$$\Delta E_p = \Delta E_0 \left( \frac{\alpha^2}{2k} \right)^x \left[ -1 + \sqrt{1 + \frac{4k}{\alpha^2}} \right]^x \dots\dots\dots 7$$

For typical values  $d_0 = 30 \text{ \AA}$  ,  $\sigma = 3 \text{ \AA}$   $x \in [1.4, 2]$  , and  $k/\alpha^2 \rightarrow 0$  ; hence

$$\Delta E_p \approx \Delta E_0 \left[ 1 - \frac{k}{\alpha^2} \right]^x \dots\dots\dots 8$$

**This can be written as**

$$\Delta E_p \approx \Delta E_0 \left[ 1 - x \frac{k}{\alpha^2} \right] \dots\dots\dots 9$$

Equation (7) implicitly contains the dependence of the peak  $\Delta E_p$  on the mean crystallite size  $d_0$ . This dependence may be different from the one suggested by Equation.(2)  $\Delta E = c/d^x$ , This is shown in figure 8.

The solid line depicts the canonical (EMT) behavior given by Equation. 2 with  $x=2$ . We plot the variation of the peak energy  $\Delta E_p$  with mean diameter  $d_0$  for a collection of spherical nanocrystallites ( $m=3$ ) with varying sizes. The variance in diameter  $\sigma$  is assumed to be  $5 \text{ \AA}$ . The dotted line represents the case when the oscillator strength is strongly dependent on the crystallite size ( $\beta=6$ ), and the broken line depicts the opposite case where the oscillator strength is size dependent  $\beta=0$ .

**If we assume the variation of the form**

$$\Delta E_p = \frac{C'}{d_0^\gamma} \dots\dots\dots 10$$

with  $\gamma_{eff} = \gamma$  is an effective exponent, we can see that in the first case  $\gamma_{eff} > 2$ , where as for the latter  $\gamma_{eff} < 2$ . Note that the size dependence of the PL peak in the broken curve is extremely weak in the region  $20-40 \text{ \AA}$ , the range considered in most experiments.

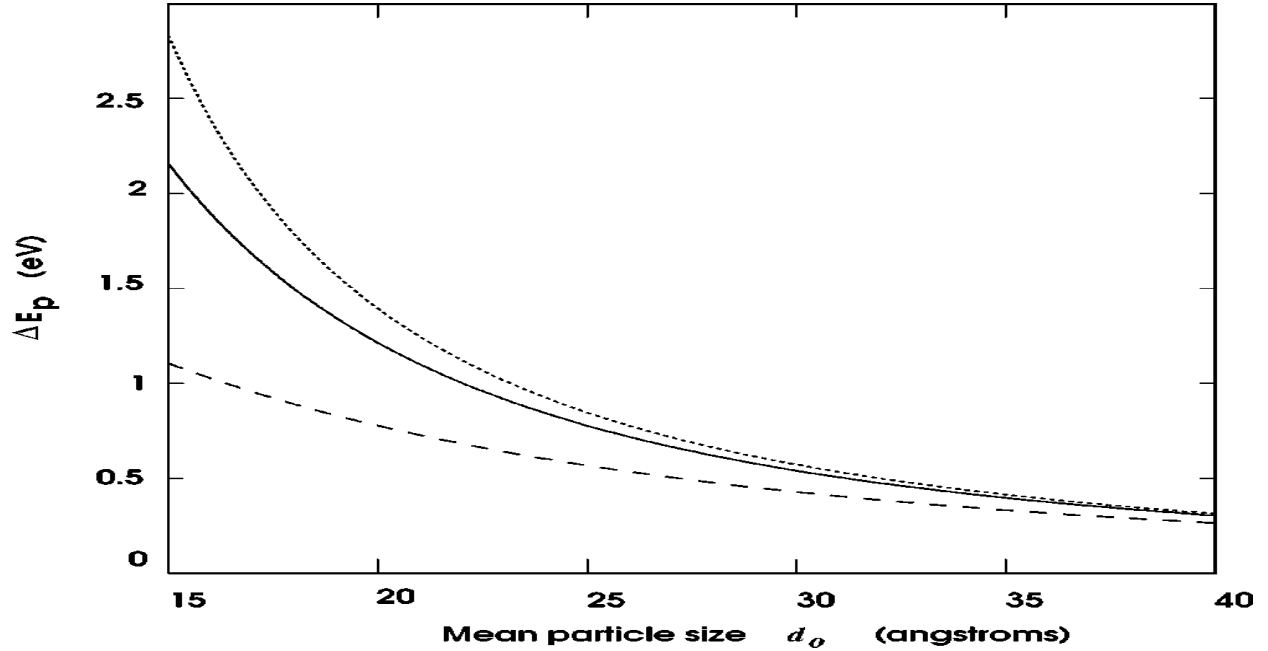


Figure 9. The dependence of the peak position  $\Delta E_p$  on the mean crystallite size, assuming a normal distribution of dots with  $\sigma = 5\text{\AA}$ ,  $x=2$ . The broken line at the bottom ( $m=3$ ,  $\beta=0$ ) shows an extremely weak variation in energy with size. The dotted line at the top ( $m=3$ ,  $\beta=6$ ) shows a strong dependence which is supra-quadratic. The distribution in the crystallite sizes results in considerable deviation from a simple  $c/d^x$  variation, which is depicted by the solid line.

case when  $m=2$ ,  $x=2$ , and  $\beta=6$ . We see that the peak positions in both cases are substantially different.

This raises questions about the assignment of the exciton binding energy, which was discussed in an earlier work. We shall discuss this issue later in this paper.

TABLE I. Table of effective exponents. The variance  $\sigma$  is in  $\text{\AA}$ , and constant  $c'$  is in appropriate units. Note the variation in  $\gamma_{eff}$  with disorder  $\sigma$  for the same  $k$  and its deviation from the assumed value of  $x = 2$ .

$k$	$\sigma$	$c'$	$\gamma_{eff}$
5	3	213.279	1.786
	5	80.307	1.541
4	3	245.967	1.823
	5	104.260	1.606
3	3	286.396	1.862
	5	140.305	1.680
2	3	337.114	1.904
	5	197.772	1.767
1	3	401.785	1.950
	5	296.668	1.871
-1	3	597.404	2.054
	5	908.810	2.166
-2	3	749.461	2.114
	5	2133.310	2.397

We now proceed to obtain an analytic expression for the exponent  $\gamma_{eff}$  by a method employed in the modern theory of critical phenomena.

First we take the logarithm of  $\Delta E_p$  to obtain

$$\ln \Delta E_p = \ln c - x \ln d_0 + x \ln \left(1 - \frac{k}{\alpha^2}\right) \dots\dots\dots 11$$

and we have

$$\ln \Delta E_p = \ln c' - \gamma_{eff} \ln d_0 \dots\dots\dots 12$$

differentiate the above equation .. with respect to  $\ln d_0$  to obtain

$$\frac{(\partial \ln \Delta E_p)}{(\partial \ln d_0)} = -x \left[ 1 - \frac{2k}{((d_0/\sigma)^2 - k)} \right] \dots\dots\dots 13$$

where we recall that  $\left(\frac{d_0}{\sigma}\right)$  is  $\alpha$ . Differentiating the above equation .. with respect to  $\ln d_0$  to

obtain yields

$$\frac{(\partial \ln \Delta E_p)}{(\partial \ln d_0)} = -\gamma_{eff} \dots\dots\dots 14$$

Equating the above two equation ....we obtain the effective exponent  $\gamma_{eff}$  as

$$\gamma_{eff} = x \left[ 1 - \frac{2k}{((d_0/\sigma)^2 - k)} \right] \dots\dots\dots 15$$

**Table 1** Optical data for Q-GaAs/4ep

Aliquot name (and time taken after injection)	PL $\lambda_{max}$ /nm	PL FWHM/nm	UV Absorption Edge (nm/eV)	Blue shift w.r.t. bulk/eV	Estimated particle diameter/nm
1 (30 min)	—	113.7	494.3/2.51	1.08	4.47
2 (1 h)	—	135.5	485.6/2.55	1.12	4.39
3 (5 h)	—	127.6	486.9/2.54	1.11	4.41
4 (1 day)	—	133.7	488.5/2.54	1.11	4.41
5 (2 days)	446.4	135.2	505.3/2.45	1.02	4.59
6 (3 days)	450	135	521.6/2.38	0.95	4.75
7 (4 days)	435.4	127.7	565.4/2.19	0.76	5.28
8 (5 days)	434.2	120.6	579.8/2.14	0.71	5.45
9 (6 days)	430.9	117.7	580.1/2.14	0.71	5.45
10	447.1	113.0	—	—	—
11	468.7	148.9	626.7/1.98	0.55	6.15

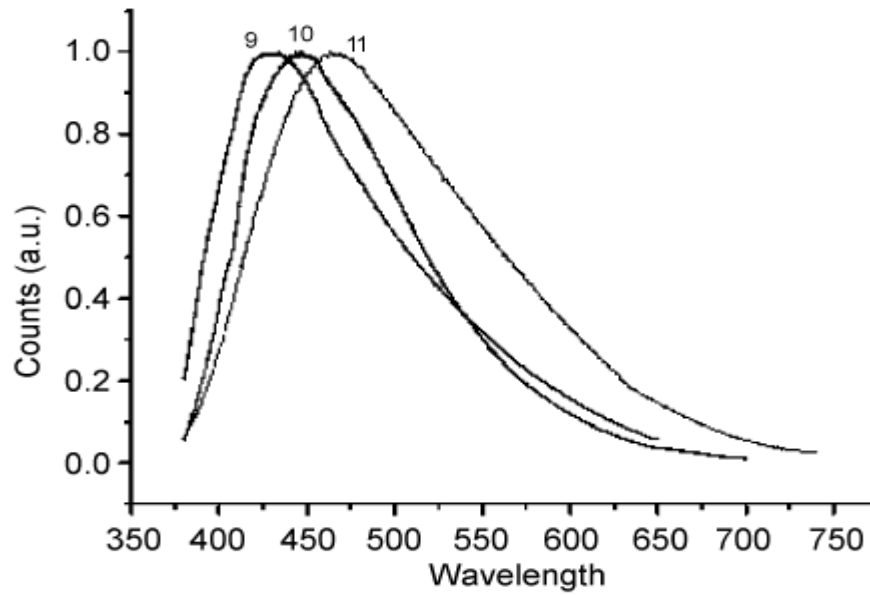


Figure 10. Emission photoluminescence spectra of Q-GaAs nanowire/4ep; aliquot 9 (after 6 days), 10 (addition of further precursor) and 11 (addition of further precursor).

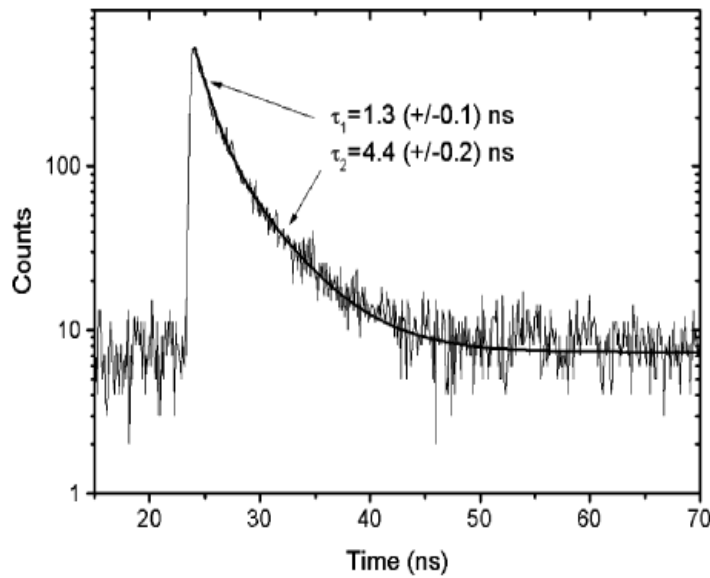


Figure 11. Room temperature TRPL data for GaAs/4ep nanowire. A good curve fit is obtained using a double exponential decay with lifetimes of 1.3 ns (37% of counts) and 4.4 ns (63% of counts).

## Outstanding models

### Quantum confinement

Among the numerous models for the PL blue shift, “quantum confinement (QC)” theory has been elegantly accepted. Efros firstly proposed, in 1982, this concept based on the experimental findings of the size effect on the blue shift in the main exciton absorption of CuCl (~ 3 nm across) nanocrystallite. The confinement effect on the band gap,  $E_g$ , of a nanosolid of radius R was expressed as:

$$E_G(R) = E_G(\infty) + \pi^2 \hbar^2 / (2\mu R^2)$$

where

$$\mu \left( 1/\mu = 1/m_h^* + 1/m_e^* \right)$$

being the reduced mass of an electron-hole (e-h) pair, is an adjustable parameter. Equation above indicates that the  $E_G$  expansion arises from the kinetic energy of the e-h pairs that are separated by a distance of the particle dimension, R, or the quantum well size.

According to the QC theory, electrons in the conduction band and holes in the valence band are confined spatially by the potential barrier of the surface, or trapped by the potential well of the quantum box. Because of the confinement of both the electrons and the holes, the lowest energy optical transition from the valence to the conduction band increases in energy, effectively increasing the  $E_G$ . The sum of kinetic and potential energy of the freely moving carriers is responsible for the EG expansion and therefore the width of the confined EG grows as the characteristic dimensions of the crystallite decrease.

Later development of the QC theory shows that the relation of  $n$  ( $n = 1.16, 1.3, 1.37$ ) fits better the size-dependent PL blue shift and the  $n$  values vary from source to source.

Nevertheless, it is important to recognize that the QC premise is indeed a very helpful first order approximation, and can be used to estimate changes in energy levels, exciton and related energies, as a function of dot size. However, at the lower end of the size limit, the QC theoretical curve diverges from the true situation that the EG can never be larger than the separation of the involved energy levels of an isolated atom.

### Other schemes

A free-exciton collision model proposed for the PL blue shift suggests that the EG expansion arises from the contribution of thermally activated phonons in the grain boundaries rather than the QC effect. During PL measurement, the excitation laser heats the free excitons that then collide with the boundaries of the nanometer-sized fragments. The laser heating the free-excitons up to the temperature in excess of the activation energy required for the self-trapping gives rise to the extremely hot self-trapping excitons (STE's). Because the resulting temperature of the STE's is much higher than the lattice temperature, the cooling of the STE's is dominated by the emission of phonons.

However, if the STE temperature comes into equilibrium with the lattice temperature, the

absorption of lattice phonons becomes possible. As a result, the blue shift of the STE-PL band is suggested to originate from the activation of hot-phonon-assisted electronic transitions. The blue shift of the STE-PL band depends on the temperature of laser-heated free-excitons that in turn is determined by the size of nanometer-sized fragments. This event happens because the temperature (kinetic energy) of the laser-heated free-exciton increases with the number of collisions with the boundary of confined regions, which tends to be higher with decreasing size of the (silica was considered only) fragments in nanoscale materials. The energy gained from laser heating of the exciton increases with decreasing nanosolid diameter in an  $\exp(1/R)$  way. Based on the analysis, Glinka et al indicated that the size-dependent PL blue shift of a nanosolid in general does not need to be related always to the QC effect.

Other phenomenological models for the blue shift in PL of nanosolids include the impurity centers, surface states, surface alloying, cluster interaction and oxidation effect. However, all the models mentioned above are good for the blue shift in the PL and cover various possible sources. These models have their limitations, however, that could explain neither change of Hamiltonian as the origin nor other quantities relating to the Hamiltonian, such as the core level shift and dielectric suppression, which should be intrinsic to nanostructures .

According to the nearly-free-electron approximation, the  $E_G$  originates from the crystal field and the width of the gap depends on the integral of the crystal field in combination with the Bloch wave of the nearly free electron,

$$E_G = 2|V_1(k_l)|, \text{ and } V_1(k_l) = \langle \phi(k_l, r) | V(r + R_C) | \phi(k_l, r) \rangle$$

where  $k_l$  is the wave-vector and .

$$k_l = 2l\pi/R_C.$$

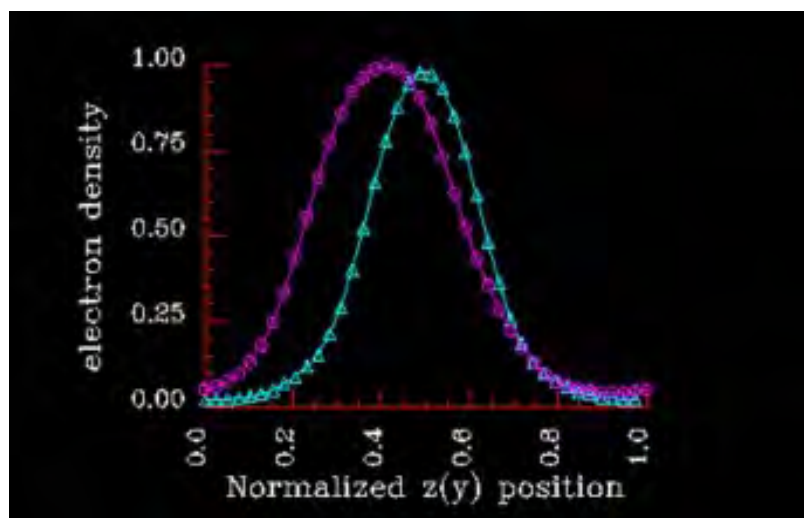
$V(r + R_C)$  is the periodic potential of the crystal,  $R_C$  is the lattice constant.

Therefore, the  $E_G$  is simply twice of the first Fourier coefficient of the crystal field.

## **VII. COMPARISON WITH EXPERIMENT**

Nanowires were grown on semi-insulating GaAs(111)B substrates. These substrates were first functionalised with poly L-lysine solution and then treated with Au colloid solution containing Au nanoparticles. We tested a range of Au colloid diameters ranging from 2 nm to 50 nm. Nanowires, catalyzed by these nanoparticles, were grown by low pressure horizontal flow MOCVD using trimethylgallium (TMG) and arsine ( $AsH_3$ ) precursors at temperatures between 330 and 500 °C. Growth times were between 1 and 60 minutes.

Field emission scanning electron microscopy (FESEM), transmission electron microscopy (TEM) and photoluminescence (PL) were employed to study the structural, crystallographic and optical properties of these nanowires



For GaAs/AlGaAs core-shell nanowires, GaAs nanowire core were grown as described above, then AlGaAs shell growth was performed for 20 minutes at  $650\text{ }^{\circ}\text{C}$  using trimethylaluminium, TMG and  $\text{AsH}_3$ .

A representative PL spectrum is shown in Figure ..... All PL measurements presented in this paper were obtained from GaAs nanowires.

PL measurements have been performed on various other nanowires corresponding to the growth

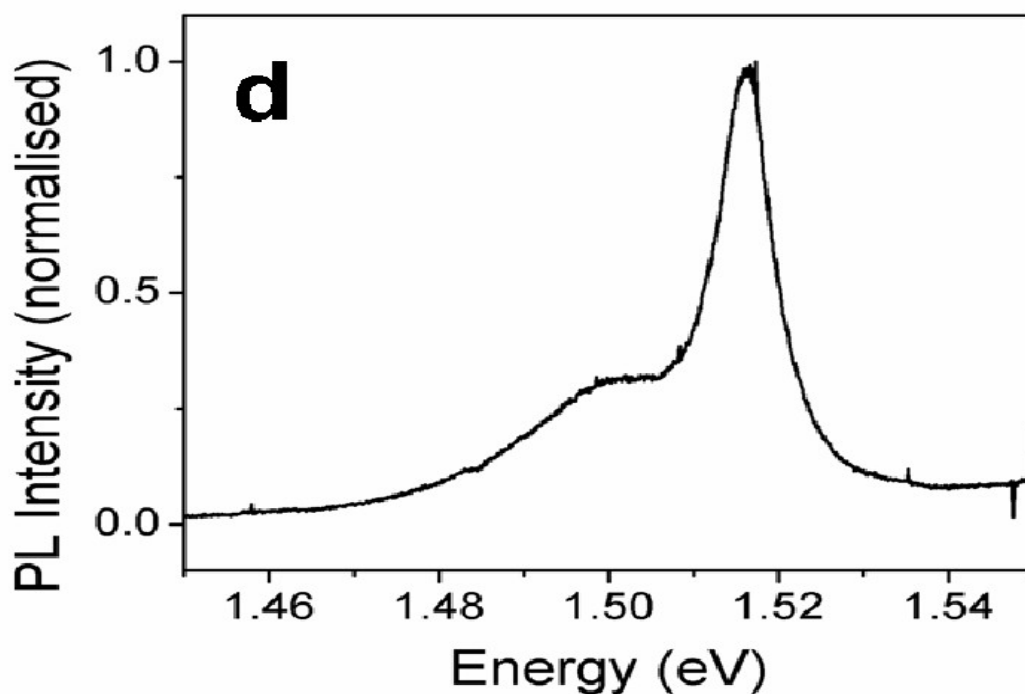


Figure 12. PL versus Energy in GaAs nanowire from the experimental data.

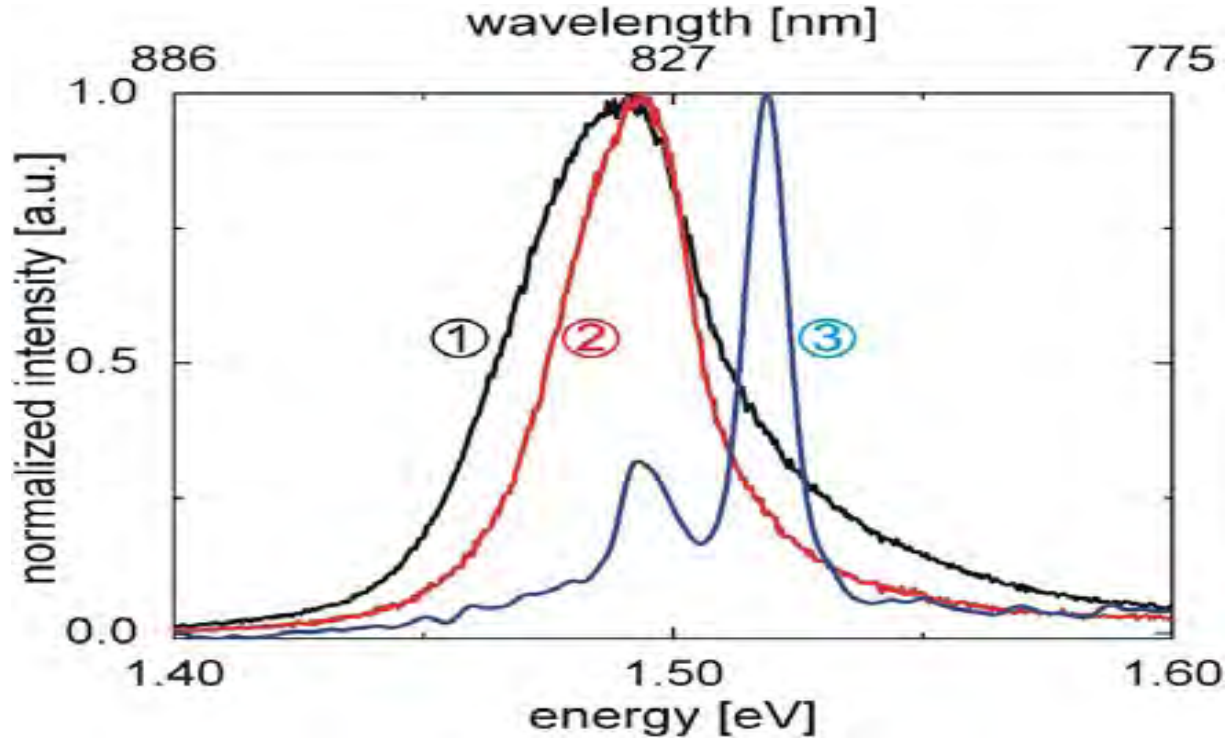


fig13 shows normalized intensity versus energy and wavelength for our study.

conditions  $\beta$  and  $\gamma$ . The spectra are in all cases very similar. Several luminescence peaks in the ranges 1.51–1.46 eV for sample  $\beta$  and 1.47–1.43 eV for sample  $\gamma$  are observed. The exact position and intensity of each peak varies from sample to sample and on the position on the nanowire. These results are in agreement with the fact that the structure varies along the axis of the nanowires. Additionally, the exact sequence of wurtzite and zinc-blende sections varies from wire to wire. In order to illustrate this, scanning confocal photoluminescence measurements of one sample of each of the  $\alpha$ ,  $\beta$ , and  $\gamma$  types are presented in Figs. 13 (a-c) respectively.

The PL emission of sample is rather homogeneous along the wire, with some variations in intensity and linewidth, but altogether consistent with pure zinc-blende GaAs. A single peak at 1.515 eV is observed, which corresponds to the free exciton line of zinc-blende GaAs. Sample  $\beta$  exhibits many more spectral features in the energy range between 1.515 and 1.46 eV. The spectral features are not homogeneous along the length. At the top part of the scan, the luminescence is brighter than at the bottom part. The free exciton peak at 1.515 eV is present in only some regions of the nanowire while lower energy peaks are observed over the whole length. The presence of the various peaks depends on the position on the nanowire.

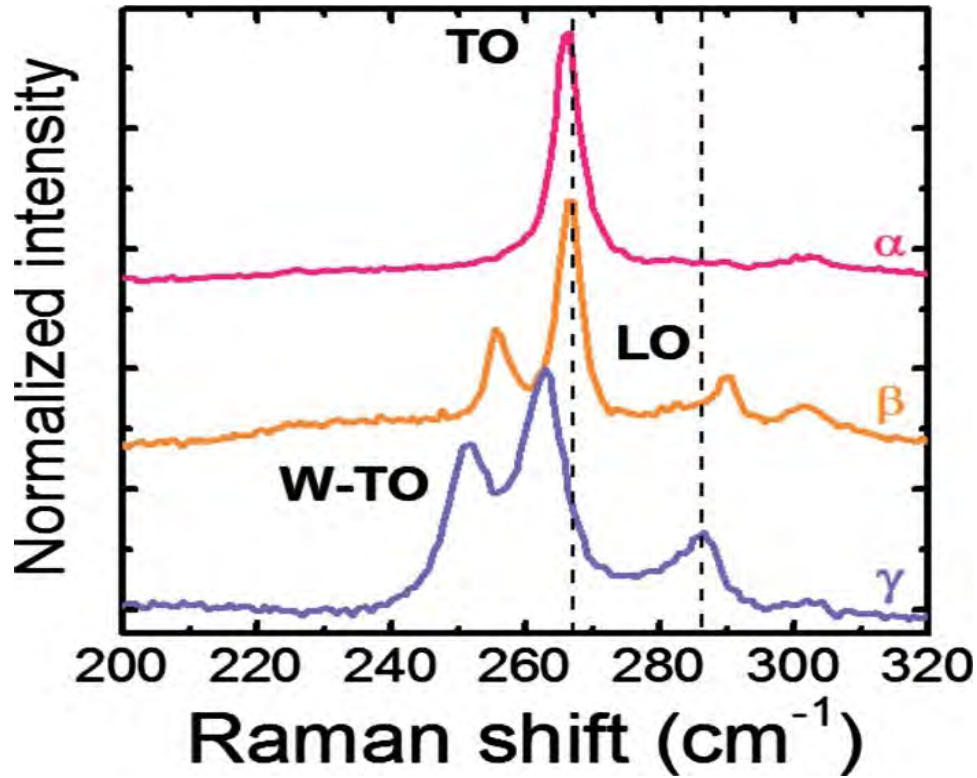


Figure 13. Intensity versus Raman shift for the three samples of GaAs nanowire discussed from the experimental data for our comparison.

### BANDSTRUCTURE: GaAs

The bandgap at 0 K is 1.51 eV and at 300 K it is 1.43 eV. The bottom of the conduction band is at  $k = (0,0,0)$ , i.e., the G-point. The upper conduction band valleys are at the L-point.

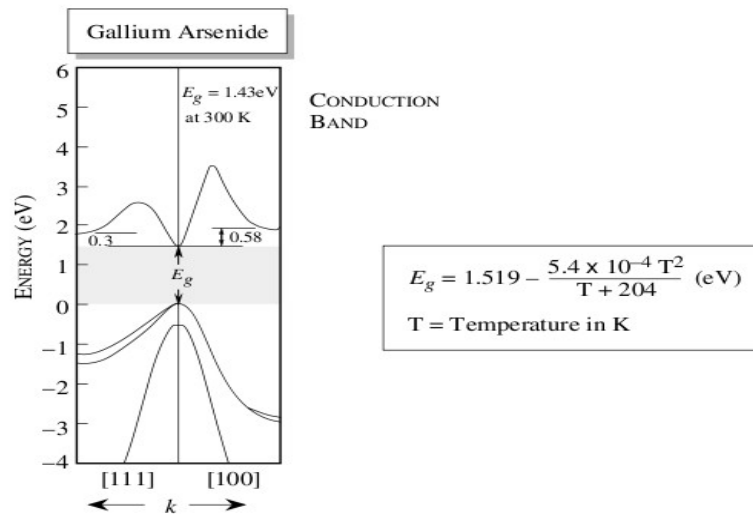
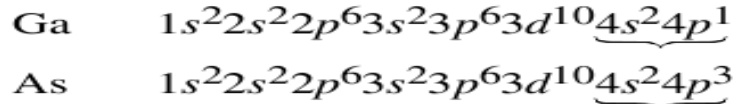
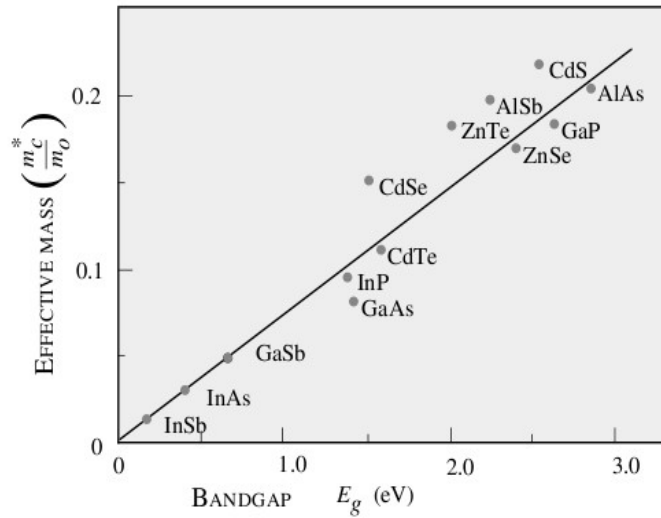


Figure 14 Energy versus wave vector in GaAs.



- CONDUCTION BAND:
- Electron mass is light.  $m^* = 0.067 m_0$
  - Upper valley mass is large.  $m^* = 0.25 m_0$  results in negative differential resistance at higher fields.
  - Material is direct bandgap and has strong optical transitions  $\Rightarrow$  can be used for light emission.
- VALENCE BAND:
- Heavy hole mass:  $0.45 m_0$ ; light hole mass =  $0.08 m_0$ .
  - Intrinsic carrier concentration at 300 =  $1.84 \times 10^6 \text{ cm}^{-3}$ .



### EFFECTIVE MASS DESCRIPTION

CONDUCTION BAND: Direct bandgap material

$$E_c(\mathbf{k}) = E_c(0) + \frac{\hbar^2 k^2}{2m_c^*}$$

with

$$\frac{1}{m_c^*} = \frac{1}{m_0} + \frac{2p_{cv}^2}{m_0^2} \frac{1}{3} \left( \frac{2}{E_{g\Gamma}} + \frac{1}{E_{g\Gamma} + \Delta} \right); \frac{2p_{cv}^2}{m_0} \sim 22 \text{ eV}$$

The smaller the bandgap, the smaller the effective mass.

SPLIT-OFF BAND:

$$E_{so} = -\Delta - \frac{\hbar^2 k^2}{2m_{so}^*}$$

$$\frac{1}{m_{so}^*} = \frac{-1}{m_0} + \frac{2p_{cv}^2}{3m_0^2(E_{g\Gamma} + \Delta)}$$

HEAVY HOLE; LIGHT HOLE:

In a simple approximation the heavy hole and light hole bands can also be represented by masses  $m_{hh}^*$  and  $m_{lh}^*$ . However, the real picture is more complex.

## CHAPTER FIVE

### CONCLUSION

Quantum confinement effect is more prominent in GaAs nanowire; in this effect, an electron can be confined in two dimension (quantum wire) .

According to the QC theory, electrons in the conduction band and holes in the valence band are confined spatially by the potential barrier of the surface, or trapped by the potential well of the quantum box. Because of the confinement of both the electrons and the holes, the lowest energy optical transition from the valence to the conduction band increases in energy, effectively increasing the  $E_G$  . The sum of kinetic and potential energy of the freely moving carriers is responsible for the  $E_G$  expansion and therefore the width of the confined  $E_G$  grows as the characteristic dimensions of the crystallite decrease.

From equation.....we can conclude:

1.  $\gamma_{eff}$  is distinct from  $x$  as long as  $k \neq 0$  Thus the quantum confinement that one observes  $\gamma_{eff}$  may be different from the calculated one ( $x$ ) irrespective of the method of calculation, whether EMT or tight binding 'TB' .
2. The exponent  $\gamma_{eff}$  is universal in the sense that it depends on the ratio  $\frac{d_0}{\sigma}$  and not separately on the mean size  $d_0$  and the variance  $\sigma$  . In other words, ensembles of equivalent disorder will have the same exponent  $\gamma_{eff}$  .
3. Note that  $k$  is usually small in the range  $[-2 : 6]$ . Hence the denominator will be positive. Thus  $\gamma_{eff}$  can be greater or less than  $x$  depending on the sign of  $k$ .
4. If  $k$  is negative ,the peak is blueshifted as Equation 8, shows,and the size dependence is more pronounced ,e.g.,  $\gamma_{eff} > x$  as the last equation shows. On the other hand, redshifted peaks will exhibit a weaker dependence.
5. As expected ,in the limit of small disorder  $\sigma \rightarrow 0$  ,the last equation yields

$$\gamma_{eff}|_{\sigma \rightarrow 0} = x.$$

Further several attempts to estimate the size of a crystallite using equation  $\Delta E = \frac{c}{d^x}$ ,

have been made in the past .Lippens and Lannoo correlated the positions of the exciton peaks to size ,and compared it favorably with their TB calculations.

Attempts to understand experimental data on the basis of calculations on single nanocrystals can be misleading .The simple model presented here,curve fitting model, outlines the pitfalls carrying out such an exercise. Properties besides the PL broadening and band shift examined herein, such as dielectric absorption, radiative life time, etc., also need to be more carefully studied in the light of our observations.

For reasons explained in detail, the band-gap variation in GaAs nanowires is rather complex, and depends on their type and geometry, diameter, relaxation, and also whether the dangling bonds of surface atoms are passivated with hydrogen.

We believe that present results are valuable for further research on GaAs and other III–V compound nanowires dealing with their doping, forming heterostructure and multiple quantum well structure, and their functionalization to get new electronic and magnetic properties.

## 5.1 APPLICATION

In searching to discover semiconductor materials metallic interconnect for new generation miniaturized electronic devices, nanostructures have been a focus of attention. Electronic devices, such as transistors based on carbon nanotubes, attracted interest in nanowires. Rodlike Si nanowires have been fabricated with a diameter of 1.3–7 nm.

It has been shown that such Si nanowire can display metallic, semiconducting, and half-metallic properties depending on their functionalization. Being an alternative to silicon based microelectronics GaAs is one of the most important materials used in semiconductor physics. Due to the high electron mobility, GaAs always carried a potential of being used in high-speed electronic devices.

GaAs/AlGaAs heterostructure have served as media for the two dimensional electron-gas studies.

Similar to bulk crystals researcher have envisioned GaAs nanowires to be a potential alternative for Si nanowires

. Recent advances in fabrication technology made it possible to grow GaAs nanowires. They are grown by metal catalysts in vapor-liquid-solid (VLS) mechanism. Generally, GaAs nanowires are grown along [111] direction in zinc-blende (Zb) structure.

The virtues of nanotechnology have combined to make the subject worthy of special emphasis in the research community and a source of new commercial products.

This has been the result of a synergistic combination of major historical technological advances, recent scientific discoveries (especially of new scientific principles), and a futuristic vision that supports widely acclaimed goals. Surprisingly complex self-assembled structures (new materials) resulting from nature's forces have been discovered and are under intense examination for exploitation. The forces lead to biological complexity, also a result of self-assembly, and are beginning to be understood. The subject has opened new scientific frontiers and has begun to redirect scientific pursuit from somewhat narrow fields of inquiry within scientific disciplines to include broader objectives related to technologies and useful materials. Aspects of the subject that make it particularly attractive for high-level support are examined. Nanotechnology as it impacts fields of electronics and information, biology, chemistry and medicine, energy, the environment, transportation, and especially that of materials, is briefly considered.

Nanotechnology as a scientific and technological thrust encompasses the best of many opportunities afforded to the scientific, engineering, and industrial communities.

The scientific opportunities appear to be considerable, industrial interest is high, and the social benefits are significant from new materials, and new products applicable to information technology, medicine, energy and the environment. It deserves support where the objectives can be justified based on their

scientific and technological merits, and it provides a vision for transitioning new discoveries to products. The only word of caution associated with this bright frontier is: Decisions must be based on sound scientific merit having experimental evidence and/or valid theoretical foundation combined with a realistic assessment of the challenges that must be met to fulfill the promise.

Nanoparticles will also be the building blocks for complex structures like nanowires and molecule electronic devices. Some of the pieces will be built into moving parts, and perhaps, one day, scientists will get around to the rampaging nanorobots.

**Tiny Is Beautiful:** Translating 'Nano' Into Practical in the hip science of ultra small nanotechnology, fantastical future possibilities like rampaging nanorobots capture the most attention, but the first fruits of the field have been more mundane: tiny bits of mostly ordinary stuff that just sit there. Yet these bits - nanoparticles - gain wondrous new capabilities simply because they are so small. Nanoparticles of various sorts are already found in products like sunscreen, paint and inkjet paper. More exotic varieties offer promise in medicine for sensitive diagnostic tests and novel treatments: the detection of Alzheimer's disease by finding a protein in spinal fluid, for instance, or nanoparticles that heat up and kill cancer cells.

## 5.2 Challenges

Overwhelming contribution has been made to the development of nanotechnology such as atomic imaging and manipulating, nanosolid synthesizing, functioning, and characterizing as well as structural patterning for device fabrication. However, consistent insight into the mechanism behind the nanosolid tunability remains yet infancy. For a single phenomenon, there are often numerous theories discussing from various perspectives. Reconciliation of all observations in a comprehensive yet straightforward way is a high challenge.

Predictable design and controllable growth of nanostructured materials or devices are foremost important to scientific and technological communities. One needs not only to understand the performance but also needs to know the origin, the trend, and the limitation of the changes and the interdependence of various properties in order to predict and control the process for fabricating materials and devices.

Furthermore, structural miniaturization provides us with an additional freedom that not only allows us to tune the properties of the solid by changing its shape and size, but also challenges us to gain quantitative information by making use of the new freedom, which is beyond traditional approaches.

## 5.3 FUTURE OUTLOOK

We have mentioned that GaAs nanowire structures with reduced dimensionality such as for example quantum wires, and quantum dots are attracting increasing attention both as object of basic research and as promising materials for the fabrication of devices with new operational capabilities that can not be attained using traditional semiconducting materials. These materials are very important and promising in the manufacture of light-emitting diodes, high mobility transistors, sensors, monochromatic light sources, wave guides, photonic studies, data storage devices and etc. The wide spread use of these materials and other related compound semiconductor materials light wave communication systems has result in intensive research in to the growth of these materials using a number of techniques.

50% energy efficient solid state Lighting will replace all conventional lighting in the next 20 years and so. This will result in a 10% reduction in global electricity use.

In the Future We need to investigate how growth parameters may be chosen to obtain high quality GaAs nanowires suitable for optoelectronic device applications.

Growth temperature and precursor flows have a significant effect on the morphology, crystallographic quality, intrinsic doping and optical properties of the resulting nanowires.

Significantly, we find that low growth temperature and high arsine flow rate improve nanowire optical properties, reduce carbon impurity incorporation and drastically reduce planar crystallographic defects. Additionally, cladding the GaAs nanowire cores in an AlGaAs shell enhances emission efficiency. These high quality nanowires should create new opportunities for optoelectronic devices.

Therefore, GaAs nanowire are very important and promising materials in the optoelectronic and microelectronic devices.

Recently, semiconductor subwavelength nanowires (NWs) have been demonstrated to show laser emission. Representative semiconductor materials fabricating NW lasers are ZnO, GaN and Cd's, etc. Such NW lasers are currently among the smallest known lasing devices, with lengths between one and several tens micrometers and diameter that can be significantly smaller than the emission wavelength in vacuum. For a single-crystalline NW, the end facets form natural mirror surface that create an axial resonator. That is, one-dimensional semiconductor NWs not only act as a gain medium but also a waveguide and a Fabry-Pérot resonator, which provide coherent feedback. The light-emitting capability of the NWs, combined with their other unique features that arise due to their one dimensionality, make them particularly interesting to consider as a candidates for components of future nanoscale photonic systems. However, most advances of NW lasers were successfully realized via wide-bandgap semiconductor materials, giving an ultraviolet or blue laser emission, and little investigation of NW lasers in near-infrared spectral range was reported. Here we describe the growth of GaAs-based NWs using selective-area metalorganic vapor phase epitaxy (SA-MOVPE) and their near-infrared lasing at 810-820 nm wavelengths, inside GaAs/GaAsP core-shell Nws.

## References

1. H.Kroemer, *proc.IEEE* 51, 1782 (1963)
2. S.M. Sze, *Semiconductor Devices: Physics and Technology*(John Wiley & Sons,New Jersey,1985).
3. INTRODUCTION TO NANOTECHNOLOGY: Charles P. Poole, Jr. Frank J. Owens (2003 by John Wiley & Sons, Inc.)
4. Size and confinement effect on nanostructures Chang Q. Sun\* School of Electrical and Electronic Engineering, Nanyang Technological University, Singapore 639798 Institute of Advanced Materials Physics and Faculty of Science, Tianjin University, 300072, P. R. China
5. [1] W.C.W.Chan ,and S.Nie, *science* 281, 2016(1998).
6. [2] Prof.Chua Soojin,A/prof Lolkian Ping , nussni focus groups .
7. [3] C.J,wang,B.Lwehrenbers,C.Y,Woo,and P.Guyyotsionnest ,*J.phys.chem.B* 108 , 9027(2004).
8. [4] M.Bruchez,M.Morene,P.Gin,S.Weiss,and A.P Alivesor : *science* 281, 2013(1998).
9. [5] D.Riabinina,F.Rosei and M.Chaker ,*Journal of experimental nano science*, vol.1,No.1,2005.
10. [6] C.N.R.Rao ,A.Muller ,A.k.Cheetham ,*the chemistry of nanomaterials* vol.2.
11. [7] Brian A.Korgel,SPIE newsroom 10.111712,1200607.0203, synthesizing Ge quantum dots and nanowires.
12. [8] A.S.Zeng,M.J.Zheng,L.MA and W.Z.Shen , *Apply.phys.A* 84, 317-321(2006).
13. [9] Young,Changjo,Hong-joo Song,Seuk-jinjoe,Hoon kim and Pyongchol,optical properties of 1 by 16 highly sensitive InP/InGaAs hetro junction phtotransis tor arrays.
14. G. C John and V. A. Singh, *Phys.Rep.*263,93(1995).
15. S.Farfard, D. Leonard, J.L.Merz, and P.M. Petroff,*Appl.Phys.Lett.* 65, 1388 (1994)
16. [14] Julie Suzanne Biteen , Plasmon-enhanced silicon nanocrystal luminescence for optoelectronic application. 2006.
17. [15] S.McGarry, *Semiconductor nanocrystal quantum dots*. 20042.
18. [16] Arturs Medvids, Riga technical university .
19. [17] M.JZheng,XYZhang,LYang,CHLiangandLDZhang. *semicond.sci.technol.*16. (2001)507-510.
20. [18] Jerry A.Simmon,*Solid state lighting*. 2008